metals

MDPI

Review

Additive Manufacturing of AISI 316L Stainless Steel: A Review

Danilo D'Andrea

Department of Engineering, University of Messina, Contrada di Dio (S. Agata), 98166 Messina, Italy; dandread@unime.it; Tel.: +39-3930209246

Abstract: Additive manufacturing (AM) represents the present and the future of manufacturing production, thanks to a new design paradigm that allows the customization of components based on the needs of the final application, all framed in a perspective of sustainable and on-demand production. It has become an increasingly popular method for manufacturing complex and custom parts, especially those made from metallic materials, such as AISI 316L. AISI 316L is a type of austenitic steel widely used in industries such as aerospace, medical, automotive, and marine due to its excellent corrosion resistance and high strength. Thanks to its physico-chemical properties, AISI 316L stainless steel is one of the most used metals for AM. In this paper, a critical review of printing technologies, microstructural defects, mechanical properties, as well as industrial applications of AISI 316L are presented based on the state of the art. Furthermore, the main challenges with AM AISI 316L techniques are discussed, such as the influence of printing parameters, surface quality, and other common problems identified in the literature. Overall, this paper provides a comprehensive overview of AISI 316L AM techniques, challenges, and future research directions.

Keywords: additive manufacturing; AISI 316L; microstructure; mechanical properties

check for updates

Citation: D'Andrea, D. Additive Manufacturing of AISI 316L Stainless Steel: A Review. *Metals* **2023**, *13*, 1370. https://doi.org/10.3390/met13081370

Academic Editor: Namhyun Kang

Received: 27 June 2023
Revised: 18 July 2023
Accepted: 26 July 2023
Published: 30 July 2023

Copyright: © 2023 by the author. Licensee MDPI, Basel, Switzerland. This article is an open access article distributed under the terms and conditions of the Creative Commons Attribution (CC BY) license (https://creativecommons.org/licenses/by/4.0/).

1. Introduction

Additive manufacturing, also known as 3D printing, is a process of creating physical components layer-by-layer starting from a digital model [1,2]. It involves building up layers of material, such as plastics [3], metals [4], or ceramics [5,6] until the final object is formed. Additive Manufacturing (AM) has its roots in the 1980s. The first 3D printing process was invented by Chuck Hull [7], who founded the company 3D Systems in 1986. Hull's process, called stereolithography, is a process that solidifies thin layers of ultraviolet (UV) light-sensitive liquid polymer using a laser [8]. The introduction of AM using metal powders occurred later in 1994 when the German company EOS commercialized a machine called EOSINT based on laser-sintering technology [9]. The steps involved in product development using rapid prototyping are shown in Figure 1.

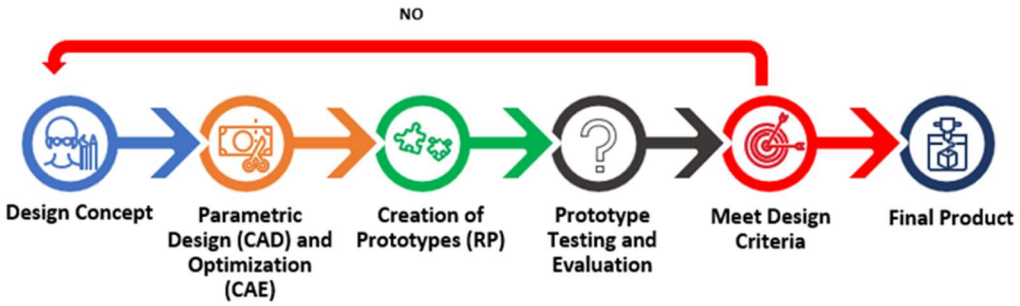


Figure 1. Product development cycle of 3D-printing process.

The first step is the digital model design of the component using computer-aided design (CAD) software. The software allows designers to create a 3D model by manipulating

digital shapes and forms. Once the object has been designed and optimized, the 3D model is prepared for 3D printing using slicing software, which divides the digital model into hundreds or thousands of layers [10].

The 3D printer must be set up and configured before printing can begin properly. This includes selecting the appropriate printing parameters that can affect the design criteria, such as the temperature and speed of the printer or the laser power [11].

After the printing process is complete, the object is removed from the printer, and any support structures are removed. The object may also need to be sanded or polished to achieve the desired finish. Compared with traditional manufacturing technology such as casting and forging, AM has has many advantages, such as:

- Customization: AM allows for the creation of complex and customized designs, like lattice structures [12,13], that cannot be easily replicated using traditional manufacturing techniques. This means that products can be tailored to specific customer needs or requirements.
- Reduced waste: AM is an additive process, meaning that it only uses the amount of material needed to create the specific part, and there are just a few waste materials, such as supports. This can significantly reduce waste and lower material costs, making the process sustainable [14–16].
- Cost-effective: For small production runs, AM can be more cost-effective than traditional manufacturing methods because traditional manufacturing technologies often require expensive molds or tooling, which are cost-prohibitive for prototyping [17,18].
- On-demand production: AM allows the manufacturer to produce parts on demand, helping to reduce costs and environmental pollution and improve supply chain efficiency. Additionally, AM reduces the risk of obsolescence, as parts can be easily updated or changed as needed [19–21].

However, many disadvantages of AM technology still exist today, including:

- Printable Materials: although in the last decade, the materials that can be used with additive techniques have increased, AM is limited to a smaller range of materials [22,23].
- Surface finish and quality: AM products are characterized by a rough surface finish [24,25], which may not be suitable for some applications, especially when the component may be affected by fatigue phenomena.
- Microstructure and mechanical properties [26]: In some cases, another disadvantage of AM is the microstructure of the printed parts, which is characterized by porosity [27], voids [28], grain growth, inclusions, and un-melted powders [29] that cause differences in material properties, such as strength, toughness, and fatigue resistance. The microstructure of printed materials is influenced by many factors, including the printing parameters [30–32], the type of material used, and the post-processing steps. It is possible to underline that, in many cases, the use of suitable printing parameters leads to the achievement of better mechanical properties even compared to traditional processes. In fact, the microstructure of a printed part can be improved through heat treatment or other post-processing steps.

Thanks to the advantages previously listed, the AM has found an increasingly large market that embraces many industrial fields, such as aerospace [33,34] or automotive [35–38], thanks to the possibility of producing lightweight components, medical field producing implants [39–42] and prosthesis [43–45] with complex shapes, and so on.

There are several 3D printing technologies available today, and each has its own strengths and limitations. Table 1 reports the most used AM technologies.

Table 1. Outline of the most used AM techniques according to ASTM 52900 [46].

Categories	Techniques	Materials	Strengths/Downsides	References
Material extrusion	Fused Deposition Modeling (FDM)	Polymers, ceramic	- Multi-material printing - Poor surface quality	[47,48]
d Vat photopolymerization	Stereolithography (SLA) Digital Light Processing (DLP)	Photopolymers Photopolymers	- Fast build speed - Good part resolution - High cost	[49,50] [51,52]
Powder bad fusion	Selective Laser Melting (SLM) Electron Beam Melting (EBM)	Metals, polymers, ceramic	- High accuracy and details - Fully dense part - High mechanical properties	[53–55]
Direct energy deposition	DED	Metals, polymers, ceramic	- Repair damaged part - Require post-processing machine	[56,57]
Binder Jetting	Binder Jetting	Metals	- Wide material selection - High porosity	[58,59]
y Material Jetting	Drop on Demand (DOD)	Polymers, waxes	- High surface quality - Low-strength material	[60,61]
Sheet lamination	Ultrasonic additive manufacturing (UAM) Laminated object manufacturing (LOM)	Metals, polymers	- High surface quality - Low cost	[62,63]

With particular reference to Metals Additive Manufacturing (MAM), one of the most studied and used materials is the austenitic steel AISI 316L, as demonstrated by the extensive scientific literature [64–68]. The extensive use of this steel for additive manufacturing is due to several factors, such as the high thermal conductivity of AISI 316L, which favors dissipating heat generated during the printing process, preventing excessive thermal gradients, and minimizing thermal stresses.

The solidification behavior of AISI 316L, particularly its solidification rate, makes it suitable for Additive Manufacturing thanks to the possibility of achieving the desired microstructure and mechanical properties.

It has compatibility with additive manufacturing techniques, including powder bed fusion (PBF), directed energy deposition (DED), and binder jetting.

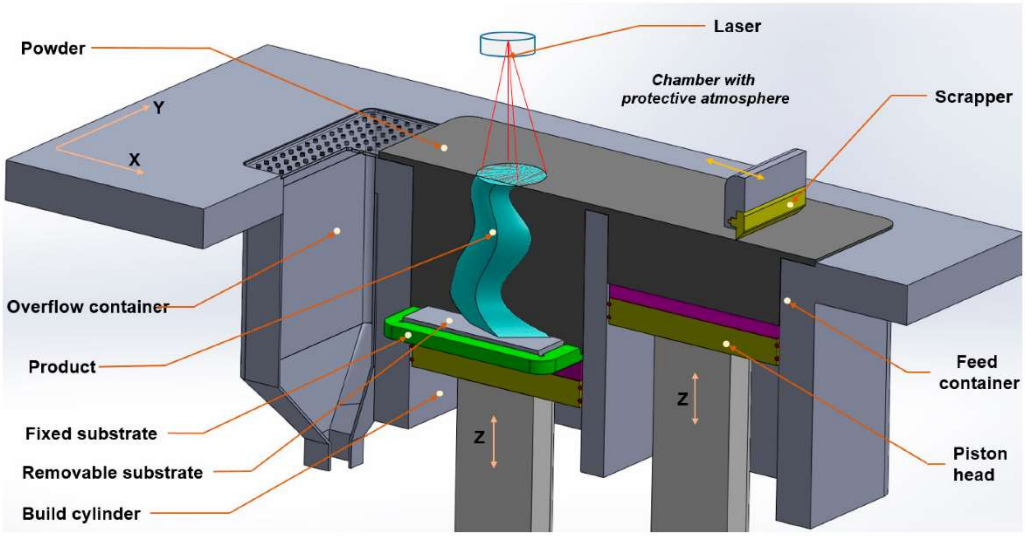
The good mechanical properties, including good strength, ductility, and corrosion resistance, make it suitable for a wide range of industries, including the aerospace field, prosthetic field, petrochemical field, and automotive field. The author has proposed a critical review of the AISI 316L state of the art, along with their applications, benefits, and the problems associated with the microstructures and mechanical properties. In addition, the main challenges with AISI 316L AM techniques, such as defect-mitigation strategy, surface quality, heat treatment, and other common problems identified from the literature, are presented. Overall, this paper provides a comprehensive outlook on AISI 316L AM techniques, challenges, and future research directions.

2. AM Technologies for AISI 316L

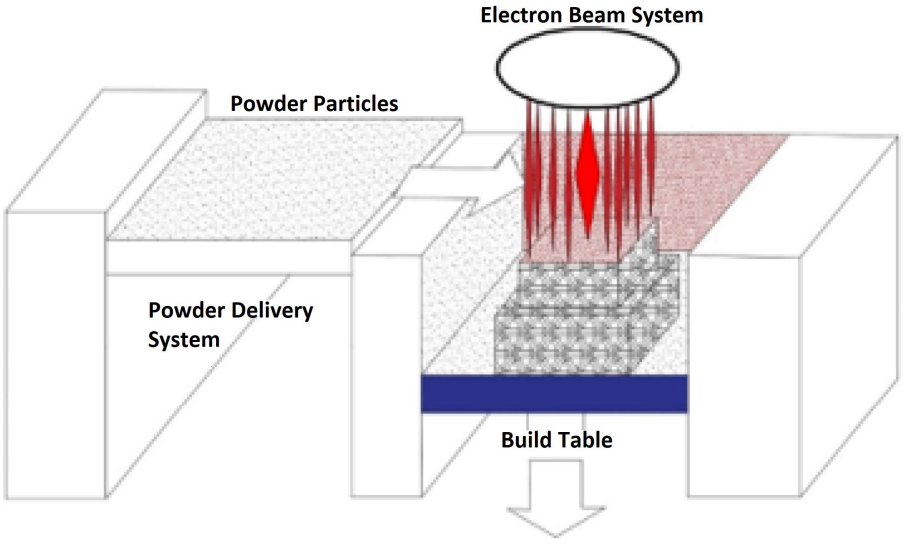
Additive manufacturing for metals, listed in the international standard ISO/ASTM 52900 [46,69], includes different types of processes, including Directed Energy Deposition (DED), Powder Bed Fusion (PBF), Fused Deposition Modeling (FDM) and Binder Jetting (BJ). Some of these processes are not yet at a technology readiness level (TRL) such as to guarantee the industrial production of components with high performance, while other technologies, such as PBF or DED, allow obtaining a full-density component with mechanical properties close to traditional processing.

2.1. Powder Bed Fusion (PBF) Technology

The PBF technology is a process that involves spreading a layer of powdered material, such as metal or plastic, over a build platform. It can be divided into L-PBF (Figure 2a) if it uses a high-powered laser to melt the powder or EB-PBF (Figure 2b) if it uses an electron beam to selectively melt the powder, fusing it together to form a solid layer. This process is repeated, with additional layers of powder being added and melted until the desired object is complete.



(**a**)



(**b**)

Figure 2. (**a**) Selective Laser Melting Technology [69]; (**b**) Electron Beam Melting Technology [70].

The L-PBF technology uses high-power lasers to melt and solidify layers of metal powder placed on the work flat [71], according to the CAD design. The laser scanning strategy, laser speed and power, layer thickness, inert atmosphere, and various other parameters are selected by the user and must be optimized for the materials and system used [72]. Although L-PBF is known to produce fully dense components with high precision in a relatively short time [73], the manufacturing process is relatively expensive and is applicable only in industries with high-value components and where higher performance may result in a reduction of costs, such as the aerospace industry.

Selective Laser Melting (SLM) is the most used technique to print AISI 316L. Suryawanshi et al. [74] have evaluated the tensile, fracture, and fatigue crack growth properties of SLM 316L stainless steel compared with those of conventionally manufactured (CM) austenitic SSs. The experimental results show that the SLM alloys' yield strength is significantly higher than that of CM 316L SS, a result of the substantial refinement in the microstructure. On the other hand, only a marginal improvement in the ultimate tensile strength and a marked reduction in ductility are attributed to the absence of stress-induced martensitic transformation common in CM austenitic SSs. Siri et al. [75] have studied the effect of high-temperature oxidation on AISI 316L stainless steel additively manufactured by selective laser melting (SLM) for 100 h at temperatures between 700 and 1000 °C in dry air and compared to that of wrought samples. Thermogravimetric analyses showed slower kinetics for SLM samples than for conventional coupons. In addition, SLM samples exhibit parabolic kinetics for all the studied temperatures, while conventional coupons present complete laws above 800 °C. Rosa et al. [76] have used the Selective Laser Melting (SLM) to produce 316L specimens including lattice structures with the aim of exploring the possibility given by additive manufacturing technologies to produce parts with increased damping capacity, especially in relation to their weight. The internal friction of bulk and lattice specimens was measured in terms of the delay between stress and deformation for different applied loads and frequencies.

As already mentioned, another PBF technique is Electron Beam Melting (EBM), which, thanks to the use of an electron beam to melt the metal powders, allows printing high-melting-point materials, such as titanium, which cannot be easily melted with other AM technologies. Even AISI 316L can be printed with the EBM technique, as demonstrated by the scientific literature [77,78]. Wang et al. [79] have presented an experimental study of process optimization of critical parameters for stainless steel 316 L parts additively manufactured via selective electron beam melting (SEBM). Tensile test results showed that most of the SEBM-built SS316L samples exhibit higher tensile strengths than the conventional cast and wrought counterparts, whereas their ductility is lower. In addition, strong anisotropic tensile properties are observed for the SEBM-built AISI 316L samples.

2.2. Directed Energy Deposition (DED) Technology

Another technology that uses AISI 316 L to produce components in additive manufacturing is Directed Energy Deposition (DED) [80–82], which, although it uses a laser or an electron beam, differs from powder bed techniques as the material is used as a wire or powder placed directly on the component (Figure 3). The advantages of using the DED are in producing large components or repairing existing ones. Moheimani et al. [83] have evaluated the role of substrate preheating on the microstructure, hardness, surface roughness, and mechanical properties of AISI 316L samples obtained by DED, confirming that the use of a preheated substrate respect to the cold one led to a lower thermal gradient, lower cooling rate, higher inclusion content, higher oxygen pick-up, and lower nitrogen pick-up that strongly affected the mechanical characteristics of the AISI 316L samples. Azinpour et al. [84] have proposed a numerical method to predict the material failure induced by porosity evolution through the micro-void growth mechanism. The performance of the numerical model is assessed via material deformation analysis, including initiation and propagation of cracks, which are found to be in good agreement with the experimental and fractographic observations from AISI 316L samples obtained by directed energy deposition (DED). On the other hand, Xu et al. [85] optimized the overlap ratio to adjust grain morphology and improve the mechanical properties of 316L stainless steel fabricated by direct energy deposition (DED). By optimizing process parameters (such as overlap ratio, laser power, and scanning speed), the penetrating-columnar-grains morphology is eliminated, and a fully dense (>99.9%) DED-316L with finer grains is achieved.

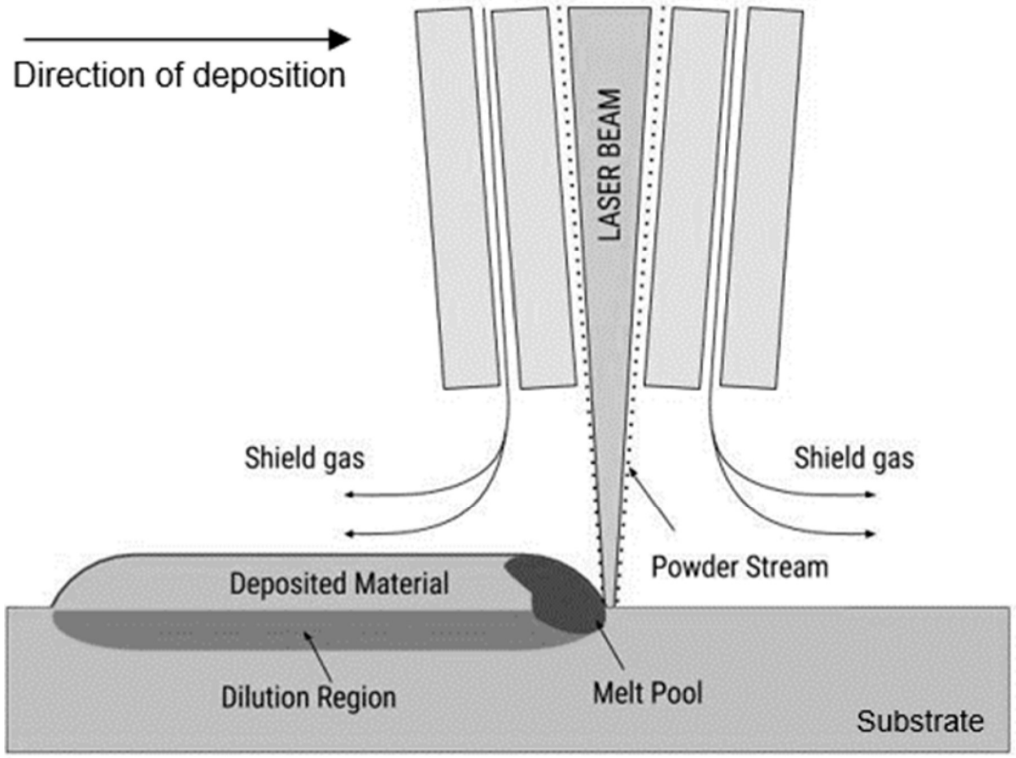


Figure 3. Process of Direct Energy Deposition Technique [56].

2.3. Binder Jetting (BJ) Tehcnology

In the binder jetting (BJ) process (Figure 4), no power heat source is used, and thus manufactured parts have no residual stresses as opposed to laser-based additive manufacturing processes. Due to the absence of rapid melting and solidification steps, this technique is becoming increasingly important in the scenario of metal additive manufacturing processes. However, this technology requires considering the effects of powder wettability with the binder and sinterability of the material to achieve desirable mechanical properties. As mentioned above for other techniques, one of the most used types of stainless steels is AISI 316L, which has been extensively manufactured using BJ, obtaining, in some cases, parts near full density and mechanical properties compared to traditionally manufactured parts [86–88]. Lecis et al. [89] have explored the effects of different processes and thermal parameters on the porosity and mechanical properties of binder jetted AISI 316L samples. The effect of the layer thickness and binder saturation were investigated at the green and sintered stages via microstructural and compositional analysis and mechanical characterization. The 316L steel produced in this work by binder jetting exhibited a fine equiaxed microstructure, tensile strength values comparable to those of cast products and superior ductility compared to other additive techniques. Cai et al. [90] have studied the application of an environmentally friendly PVA-based binder with high water content (up to 80%). The developed binder with high wettability enabled good bonding between the powder layers. A fully dense AISI 316L part with low carbon and oxygen residuals was obtained by continuous debinding–sintering treatment. Fine equiaxed grains were found in the sintered sample, leading to a high ultimate tensile stress and elongation.

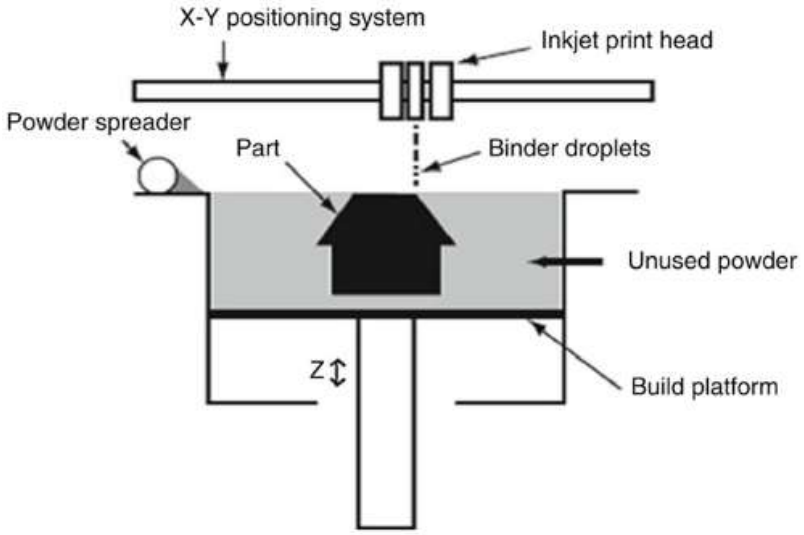


Figure 4. Printing process of binder jet [86].

2.4. Fused Deposition Modeling (FDM) Technology

In recent years, in addition to the common methods like PBF and DED, low-cost AM techniques have been applied to produce metal components, including Fused Deposition Modeling (FDM) (Figure 5), which is typically used with polymeric materials. Using a metal–polymer composite filament characterized by a homogenous mixture of metal powders and polymeric matrix, it is also possible to obtain components of complex geometry, which, however, require a post-processing phase to eliminate the polymeric part. Also, in this case, AISI 316L is widely used with FDM technology, as demonstrated by the scientific bibliography reported [91,92]. Carminati et al. [93] have investigated the mechanical properties of AISI 316L samples printed using the metal FDM process. The test results have indicated that metal material extrusion seems to be a promising technology for producing non-critical metallic parts that require good mechanical properties, good corrosion resistance, and complex shapes, such as chemical tanks, heat exchangers, and medical instruments. Quarto et al. [94] have investigated the possible influence of some relevant FDM printing parameters on dimensional shrinkage and bulk density of the metal samples. The experimental analysis was conducted by means of a statistical method and showed that the samples with the worst bulk density showed a higher percentage of opened porosity, while the percentage of opened porosity for samples with the best combination of process parameters was less than 3%.

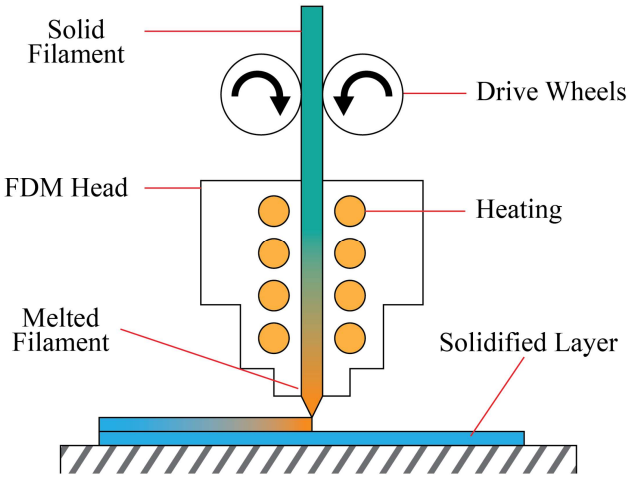


Figure 5. Process of Fused Deposition Modeling Technique [95].

2.5. Emerging Technologies

There are other techniques to print AISI 316L, like the wire arc additive manufacturing process (WAAM) [96,97], but they all have advantages and disadvantages with respect to the quality of the result in terms of the microstructure [98], mechanical properties, presence of residual stresses due to fusion processes, as demonstrated by Rodrigues et al. [99], and so on. Ozsoy et al. [100] have studied the combination of wire arc additive manufacturing (WAAM) and laser powder bed fusion (L-PBF) utilizing dissimilar metals. In particular, the authors have performed the deposition of AISI 316L stainless steel on previously L-PBF manufactured 17-4 PH stainless steel using the WAAM process. Tensile tests conducted on the specimens extracted from the L-PBF/WAAM interface showed a ductile fracture from the WAAM region, validating the strength of the interface. Hietala et al. [101] have evaluated the mechanical properties of AISI 316L printed via the WAAM process. They have shown that the tensile strength in the deposition direction was greater than in the build direction, which is explained by the anisotropy generated in the deposition. Furthermore, the results revealed that the fatigue limit of the WAAM 316L is comparable to that of 316L sheet metal. Table 2 reports a comparison between the different AM technologies used to print AISI 316L components in terms of mechanical properties, microstructure, and cost.

Table 2. Effect of AM technologies on microstructure and mechanical properties.

Techniques	Mechanical Properties			Microstructure	Ref
	Yield Strength (MPa)	Ultimate Strength (MPa)	Hardness		
DED	352	536		Columnar and equiaxed grain	[102]
EBM	253	509		Columnar grain microstrutture	[103]
SLM	172	482	77	Columnar grain microstrutture	[104]
FDM	142	427		Layered microstructure	[92]
BJ	214	517	66	Fine equiaxed grain microstructure	[86]

The following paragraphs are dedicated to the analysis of the microstructure of the components obtained by AM, the mechanical properties, and the fields of application. It is necessary to underline that despite the large growth of additive technologies and their application, many challenges still remain to obtain products equivalent to those obtained with traditional methods.

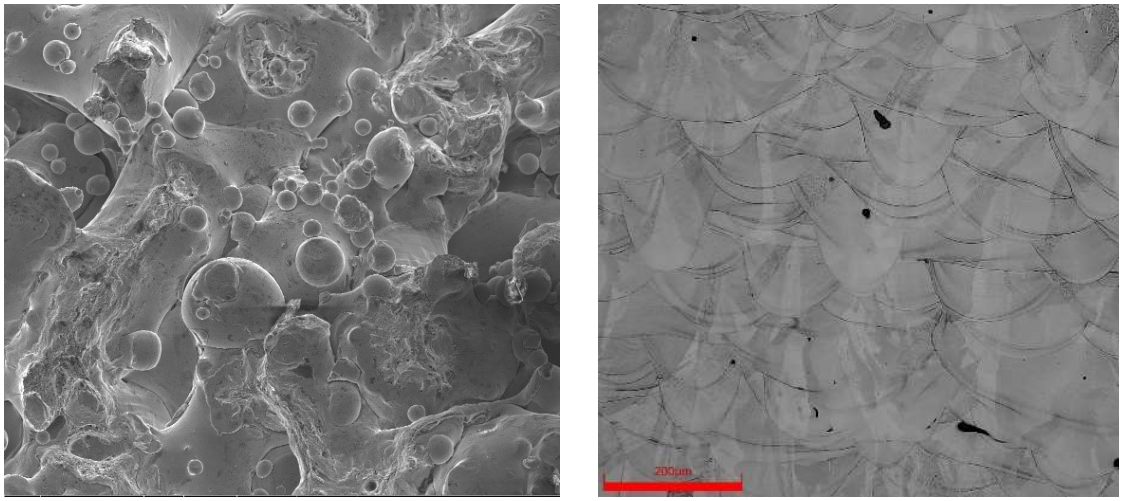
3. Microstructure Defects in AM AISI 316L

Although metal additive manufacturing has become widespread in recent years, becoming an alternative to traditional processes on certain occasions, it is still in its early stages of development, and the fundamental processing–microstructure–property relationships are not fully understood by researchers and manufacturers. Without optimization of parameters and printing conditions, defects can often arise in parts produced with AM, leading to failure of the components thus produced. The microstructure has a direct effect on the physical and mechanical properties of a material, and several studies have been conducted on the correlation between the microstructure and the effects of manufacturing parameters [85,105,106]. In this paragraph, the author has proposed an overview of the typical defects that occur in the austenitic steel AISI 316L, also underlining the influence of the different additive manufacturing techniques on the microstructure features.

3.1. Lack of Fusion and Keyhole Collapse

One of the defects that most affect the metal structures obtained by additive manufacturing is the lack of fusion (LoF) [107,108]. Especially for techniques using layer-by-layer deposition (PBF and DED) and localized melting, these defects can occur and affect the structural integrity and mechanical properties of the component. Lack of fusion (LoF)

(Figure 6) is often due to insufficient laser energy input, and defects form where the layer is not fully fused with the underlying layer. In many cases, an LoF defect contains numerous un-melted metal powders, as shown in Figure 6a [109]. There are two types of LoF defects: (1) defects with un-melted metal powders in Figure 6a, and (2) poor bonding defects due to insufficient molten metal during a solidification process, as shown in Figure 6b.



(**a**) (**b**)

Figure 6. Lack of fusion (LoF) defects: (**a**) un-melted metal powder; (**b**) bonding defects [110].

Mukherjee et al. [111] have developed a methodology to predict and prevent these defects based on a numerical heat transfer and fluid flow model for the laser powder bed fusion (PBF) additive manufacturing (AM), while Khairallah et al. [112] have demonstrated the significant effect of the recoil pressure and Marangoni convection in laser powder bed fusion (L-PBF) of 316L stainless steel, using a three-dimensional high fidelity powder-scale model to reveal how the strong dynamical melt flow generates pore defects, material spattering, and denudation zones. If too high a laser power density is used in the melting process, there is a risk of developing a keyhole defect (Figure 7). Without careful control of keyhole mode melting, keyholes can become unstable and repeatedly form and collapse, leaving voids within the deposit consisting of trapped vapor [113,114]. These pores act as stress concentrators and have a negative effect on the mechanical behavior of the material [115].

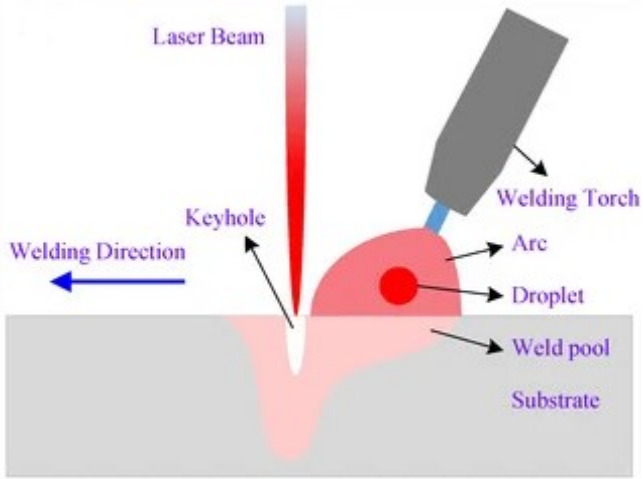


Figure 7. Keyhole defects due to the Hybrid Laser Arc Welding process [116].

3.2. Gas Porosity

The defects classified as porosity are essentially of two types. The first is the porosity induced by lack of fusion (LoF), which has already been analyzed in the previous paragraph, while the second type of porosity is induced by gaseous inclusions and can be recognized by its spherical shape (Figure 8). AM techniques using laser methods (SLM) often employ an inert shielding gas to prevent contamination of the molten pool or hot solidified metal, while in the case of an electron beam (EBM), it is performed in a vacuum or under an inert gas such as helium (He). Obviously, inert gases are insoluble in liquid metals [117], and this is often the cause of porosity. However, depending on the type of alloy used, it may be better to adopt one type of gas rather than another, as demonstrated by Elmer et al. [118], who have shown in the case of austenitic steels that using nitrogen (N2) reduces the porosity compared to the use of argon (Ar).

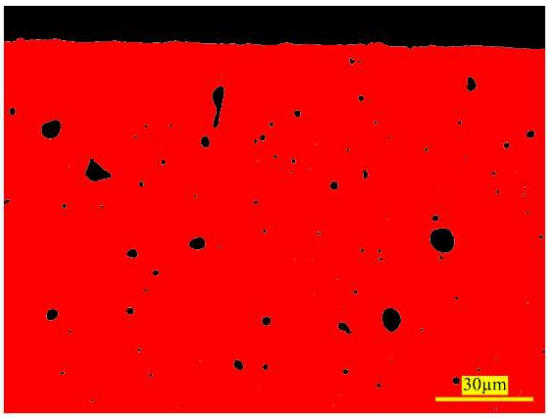


Figure 8. Gas porosity in As-built AISI 316L specimen detected by optical microscopy [119].

There are several ways to study the percentage porosity of a material. The Archimedes method [120] is the simplest non-destructive method for measuring the porosity of an entire specimen. However, to study the shape, size, and distribution of pores, it is necessary to use methods such as light microscopy, electron microscopy (SEM), or computer tomography. Ziółkowski et al. [121] have examined the possibility and accuracy of the application of the non-destructive XCT method for discontinuity and porosity detection in parts made of 316L stainless steel powder produced by SLM and have demonstrated that the accuracy of the XCT method strongly depends on the size of the samples analyzed. Jaskari et al. [122] have evaluated the effects of melting parameters and surface quality on the bending fatigue strength of SLM-manufactured AISI 316L austenitic stainless steel. Two sets of specimens were manufactured, changing printing parameters, and the specimens were heat-treated to relieve the residual stresses. They have found that although the higher strength of the low-energy-density specimens increased the fatigue limit, the surface finish did not have any effect on it due to a high amount of porosity at sub-surface layers masking the effect of surface polishing.

3.3. Surface Quality

As is known, the surface quality affects the mechanical properties of the component, in particular the fatigue properties [123] and the tribological behavior, but it also affects geometric aspects such as dimensional tolerance. Factors contributing to surface quality for powder-based systems include the alloy type, powder shape, size and morphology, printing direction, as well as laser or electron beam focal spot sizes and other process and design parameters. As stated above, wire-based processes with high deposition rates and capable of producing large components require large molten pools and feature large layered weld beads with correspondingly rough beaded surfaces. Shapes deposited using wire feedstock often require machining to achieve the desired net shape, while powder-based processes often produce shapes and features that require little finishing to achieve

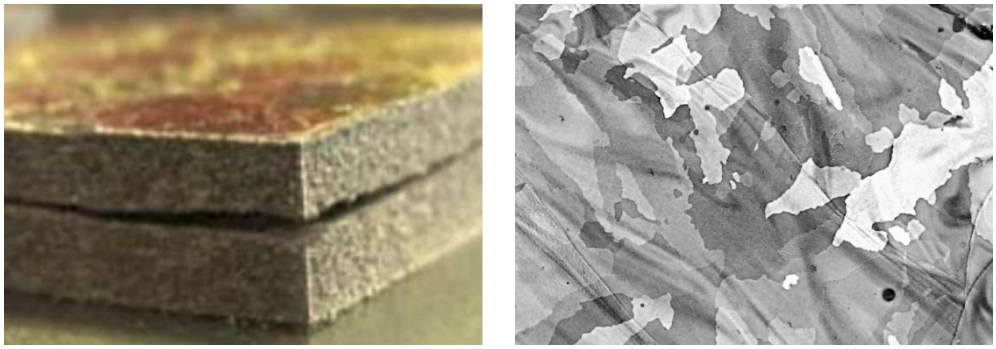
a functional form [113]. Furthermore, even down skin surfaces represent critical areas for the accumulation of defects, most often due to printing conditions (Figure 9). Solberg et al. [124] have investigated the fatigue behavior of additively manufactured (AM) 316L stainless steel related to internal porosity and surface roughness. They found that at low applied load levels and a high number of cycles, fatigue is initiated from defects in the surface region, while for high load levels, fatigue is initiated from internal defects.



Figure 9. Un-melted powders concentration on down skin surface of AISI 316L specimen.

3.4. Solidification Cracking and Residual Stresses

Residual stresses and thermal deformations are a direct consequence of AM technologies, which involve the deposition of powders or liquid metal on a previously deposited layer that is relatively colder. Residual stresses represent one of the main problems of the technology, as they represent an intrinsic limitation of the additive deposition method and can lead to part distortion, loss of geometric tolerance, and delamination of layers during deposition (Figure 10a) [125,126]. Simson et al. [127]. have investigated the effect of residual stress on austenitic stainless steel AISI 316L obtained through selective laser melting (SLM). They have evaluated that at sufficiently large distances from the top surface, the stresses in the area of the edge layer initially increase strongly and then decline again. The value and orientation of the resulting main stress components are dependent on the examined layer. They also showed that at samples with a relative structural density of >99%, the residual stress values are independent of the applied energy density. Another important aspect affecting the mechanical properties of the material is that during the additive manufacturing of AISI 316 L stainless steel, the heating and cooling cycles from selective laser melting are responsible for the grains' growth (Figure 10b) and the grain anisotropy in the "as built" condition [128,129].



(**a**) (**b**)

Figure 10. (**a**) Delamination of layers during printing phase [130]; (**b**) excessive austenitic grain growth.

Identifying appropriate strategies, such as the substrate preheat temperature, to mitigate residual stresses and stress-induced problems remains the major guiding goal for both computational and experimental studies [131–133].

3.5. Influence of Printing Parameters and Mitigation Strategies

Printing parameters play a crucial role in additive manufacturing (AM) processes [134–136]. These parameters determine the quality [32], accuracy [137], and mechanical properties of the printed components [110]. By changing the printing temperature, laser power, deposition speed, extrusion/deposition temperature, cooling system, infill pattern, printing orientation, and so on, it is possible to affect the final result in terms of layer adhesion [48], wall thickness, structural density [94], surface quality [119], anisotropy of mechanical behavior, and so on. It is important to point out that the impact of each parameter varies depending on the specific AM technologies [138], materials, and desired outcomes. Experimentation, iteration, and adjusting the parameters based on feedback and results are essential for achieving the desired quality and properties. Defect identification and mitigation is an important aspect of metal additive manufacturing to improve part quality and performance. Referring to AISI 316L AM technologies, as discussed by Mostafaei et al. [139], the printing parameters are associated with the formation of defects during the printing process. There are three main groups, including powder spreading dynamics and anomalies, steady-state conditions for defect generation, and location-specific conditions for defect formation in the metal AM process. The first issues occur during the powder dispensing step, where defects formed on the bed of the powder and bed quality, such as uniformity and powder packing density, are affected. The second and third kinds of defects form during heat source–powder interaction. If a steady-state behavior of the vapor depression is considered in the melt pool area, three main defects may be generated, such as LOF and keyhole pores, which all mostly depend on the laser power and scan speed. However, the AM processes necessarily contain many areas where these conditions are no longer true. Thus, other defects and issues may form under non-steady-state conditions, such as residual stress, cracking and delamination, geometrical defects, dimensional inaccuracy, surface roughness, microstructural inhomogeneities, impurity and inclusion formation, and loss of alloying elements. Table 3 reports the typical defects in AM AISI 316L and the mitigation strategies.

Table 3. Defect type and mitigations.

Techniques	Defect Type	Mitigation Strategies	Ref
DED	Porosity and less integral metallurgical bonds	- Increase interlayer time intervals	[80]
EBM	Strain-aging cracking	- Solutionizing treatment for base metal	[140]
SLM	Residual stress and cracking	- Adopting high preheat temperature - Using short scan vectors	[141]
SLM	Cracking	- Developing a process window for hatch spacing and laser exposure time - Undergoing HIP post-treatment	[142]
BJ	Surface roughness	- Boron additive addition	[143]
BJ	Surface roughness	- Mono-size powder	[86]

4. Mechanical Properties

The mechanical properties represent the main indicator for evaluating the quality of the material, and in particular, in the case of materials obtained in additive manufacturing, the comparison of their mechanical properties with those of the same material obtained with traditional methods [144] allows us to evaluate how much the printing process influences the performance of the final product. As pointed out in the previous paragraph, the mechanical properties of the AM material are strictly related to the microstructure and, consequently, to the printing parameters. In this paragraph, the author documents how the material properties such as hardness, ultimate tensile strength, corrosion resistance, or fatigue life of AM AISI 316L are influenced by the structural defects induced by the type of additive manufacturing technique used.

4.1. Hardness

The hardness of AM AISI 316L depends on various factors, such as the specific additive manufacturing process, process parameters, post-processing techniques, and the quality of the final part. In general, AM AISI 316L tends to exhibit comparable or slightly higher hardness compared to conventionally manufactured 316L stainless steel.

Britt et al. [145] have evaluated the hardness in different AM 316L specimens, showing no significant variation in hardness changing the thickness of the specimens maintaining the same printing parameters. However, specimens obtained with different process parameters displayed a statistically significant variation in hardness compared to the other parameter sets. Bartolomeu et al. [146] have shown variation in hardness between SLM, hot pressing, and conventional casting AISI 316L specimens. In particular, SLM specimens showed a higher value in hardness compared to the other techniques. The same results have been confirmed by Sun et al. [147], who performed microhardness tests on solid and completely fused regions, which showed that all the SLM samples possess a similar hardness value of 230–240 H, which is higher than the hardness of the standard bulk AISI 316L stainless steel (185 HV).

4.2. Corrosion Resistance

Also, for corrosion resistance, the printing process introduces intrinsic problems to the technology that are not easily solved. For example, one of the criticalities of the current L-PBF technology, which is not easily eliminated, concerns the mechanism of the "vapour pressure" of the elements, which determines the selective vaporization of the elements, such as Chromium (Cr) and Manganese (Mn) in the AISI 316L, resulting in different chemical

compositions between the surface and the core of the piece, and also different from the powder [112,148,149]. Santonocito et al. [110] have demonstrated the difference in corrosion behavior between the AISI 316L specimen obtained by the turning process and the AM ones. As shown in Figure 11, the polarization curve of AM AISI 316L (red curve) never reaches passivation, thus demonstrating that the material is subject to corrosive phenomena.

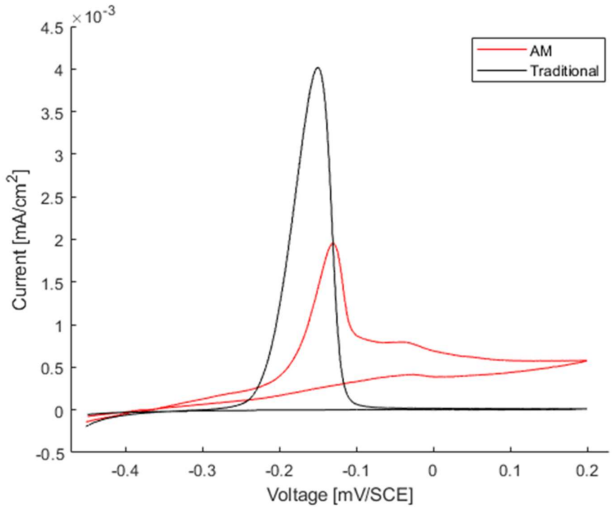


Figure 11. Difference in corrosion behavior among AM and traditional AISI 316L specimens [110].

Bassis et al. [150] have studied the effect of a slow strain rate on the stress corrosion resistance of AISI 316L produced by the wire laser additive manufacturing process, showing that the corrosion performance of the WLAM samples is lesser than the counterpart AISI 316L alloy, as expressed in the potentiodynamic polarization analysis. Bae et al. [151] have investigated the corrosion resistance of L-PBF AISI 316L stainless steel and the effect of heat treatment in comparison with cold-rolled AISI 316L. As it has been demonstrated, the SLM-fabricated AISI 316L materials with sub-grain cells have excellent corrosion and oxidation resistance due to their higher chemical stability compared with conventional cold-rolled SS316L. However, due to the post-heat-treatment, an amount of the local alloy element concentrates at the sub-grain cell are removed, and the stable amount of Cr2O3 for the oxide film formed on the surface is reduced, thereby reducing corrosion and oxidation resistance.

4.3. Tensile and Fatigue Properties

The mechanical response of the materials, in particular, the ultimate tensile strength and fatigue behavior, are among the most investigated characteristics because they provide information on the reliability and durability of the material, and in particular, with reference to additive manufacturing, they represent a quality index of the printing process both in comparison with traditional methods and as a comparison between the various technologies. As mentioned several times in this review work, the materials obtained by the additive technique are subject to structural defects that affect the mechanical properties. These flaws are not only intrinsic to AM but often change according to the AM technology used. As pointed out by Debroy et al. [113], in AISI 316L made by DED, the ultimate tensile strength decreases with increasing linear heat input, but no clear trend is found in ultimate tensile strengths as a function of the volumetric heat input. Lower linear heat inputs result in smaller melt pools, higher thermal gradients, and therefore fast cooling rates and fine microstructures, leading to higher ultimate tensile strengths compared to components made with higher linear heat inputs [102,152]. In AISI 316L made by PBF, no clear trend can be identified in ultimate tensile strengths as a function of linear or volumetric heat input. In the PBF technique, the thermal history of the components being fabricated depends on the scan strategy, which is not easy to detect. However, scan strategies vary between studies based on multiple samples being fabricated on the same build plate and

the orientation of the samples [153,154]. The variation in scan strategy, as well as any variation in laser spot size or build preheating, is at least partially responsible for the lack of clear trends. Werner et al. [155] have compared the fatigue properties (high and low cycle fatigue) between the additively manufactured AISI 316L (L-PBF) and the wrought steel both subjected to heat treatment, showing higher fatigue limit and better finite life performance of AM AISI 316L. Likewise, Ponticelli et al. [156] have investigated the L-PBF AISI 316L specimens with a quasi-static tensile test, proving that L-PBF specimens have lower elastic modulus but higher ultimate tensile strength than the original bulk material, whereby the results evidence a strong anisotropy related to the building orientation. Internal defects and building orientation are found to strongly affect the fatigue behavior, with the fatigue limit lowered from 50% of the ultimate strength of the bulk material down to 20% for the L-PBF specimens. Blinn et al. [157] have evaluated the relationships between AM processes, the microstructure, and the mechanical properties of AISI 316L material manufactured using different AM and traditional processes. The authors showed that the austenite stability and building directions affected the fatigue properties of the different AISI 316L specimens, while no significant influence of the heat treatment on the anisotropic behavior of the AM-specimens was assessed. To evaluate the fatigue behavior of AM AISI 316L, energy methods have also been used, as reported by Santonocito et al. [158], who used the thermographic method (TM) to derive in a very rapid way the SN curve and fatigue limit of the material monitoring its energetic release during fatigue tests.

5. Applications

AISI 316L stainless steel is the most commonly used austenitic stainless steel after AISI 304L stainless steel. As investigated by Kernel et al. [159] in a study based on an electrochemical comparison between these two steels, the addition of molybdenum provides greater corrosion resistance than 304L. Therefore, AISI 316L finds its main application where the resistance to localized attack by chlorides and to general corrosion by reducing acids, such as sulfuric acid, is of fundamental importance. This material is commonly used in the petrochemical and chemical industries, where corrosion resistance at high temperatures is required [160]. In fact, due to its superior strength, resistance to high temperatures, and anticorrosive qualities, particularly in harsh environments, it is widely used in nuclear reactors [161–165], boilers [166–168], pipelines [169,170], heat exchangers [171–173], furnaces [174,175], and the oil and gas and chemical industries [176]. Due to the high mechanical strength and corrosion resistance, AISI 316L stainless steel is also used as a filter in food processing industries, where the stainless steel filters are subjected to severe conditions associated with the removal of solid particles from fluids [177–179]. In the pharmaceutical industry, stainless steels like AISI 316L are cheap and easy to process and, in addition, enhance structural and corrosion resistance. Its main application regards medical devices and implants, such as artificial joints, where the corrosion process due to the body's fluid environment results in accelerated deterioration of the surface performance of the implant [180–182]. AISI has also been extensively used in the biomedical industry due to its excellent biocompatibility and corrosion resistance [183,184]. AM AISI 316L has shown promising results in the production of complex geometries and personalized biomedical implants, such as orthopedic and dental implants, enabling better patient-specific fit and function [185–188]. Considering also both onshore and offshore marine applications, AISI 316L stainless steel has played an important role in fabricating thousands of tonnage marine structures and machinery successfully over the past few decades [189]. Materials like that are mainly used in the fabrication of offshore oil and gas pipelines [190–193], offshore ocean mining machinery [194,195], chemical tankers in ships [196,197], as well as in architecture offshore environments like the construction of bridges in cold countries. The recent trends regarding Battery Electric Vehicle (BEV) and fuel cells make AISI 316L also suitable for automotive applications [198,199]. Taking into account all the considerations above and the available literature, Figure 12 summarizes the main filed of applications in which AISI 316L takes place.

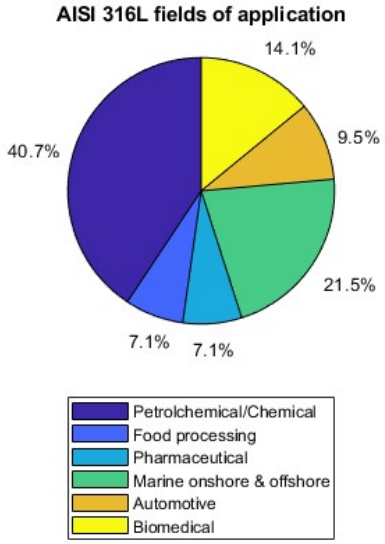


Figure 12. Fields of application of AISI 316L.

6. Challenges and Future Trends

AM is a process of creating parts from a 3D CAD model. As extensively highlighted in this work, AM has many potential advantages but also numerous barriers and challenges that researchers and manufacturers are trying to solve. Regardless of the type of technology used, AM represents a disruptive technology from the point of view of the evolution of the productive idea. The ability to create geometrically complex and customizable shapes and to easily modify the prototypes by acting on the CAD drawing represents, together with the savings in terms of material used and, therefore, sustainability, the innovative and advantageous aspects of AM technology. However, today, there are still numerous challenges that must be addressed and overcome by the scientific community and manufacturers, including:

- The high manufacturing time and therefore the low production volumes, which make AM suitable today for particular markets such as aerospace or prosthetics.
- The surface quality of the finished components, which is a function of the layer resolution. While a higher layer resolution provides a better surface finish, it greatly increases the total build time.
- The limited variety of materials that can be used in AM units, with the difficulty of printing multiple materials simultaneously, limit the use of this technology to particular sectors.
- The need for post-processing treatments to eliminate excess material, supports, residual stresses and, where possible, improve the surface finish, represent a barrier to AM accessibility.

Future efforts of the scientific community could focus on the search for appropriate modifications to the printing process to mitigate or eliminate the effects of the building direction and, therefore, the anisotropy of the printed components. To meet the requirements of advanced applications, the AM product must have superior qualities in terms of internal residual stresses of the material, surface finish, internal defects, and modification of the chemical composition of the alloy due to the printing process. In a historical period in which raw materials are increasingly difficult to find, and the sustainability of production has become one of the main objectives, the hoped-for future for this technology is an on-demand production which makes it possible to make the industry sustainable from the point of view of the reduction of waste of raw materials, of overproduction and storage of components, and of environmental impact associated with the reduction in transport.

Funding: The author(s) received no financial support for the research, authorship, and/or publication of this article.

Data Availability Statement: The data presented in this study are available on request from the corresponding author.

Conflicts of Interest: The authors declared no potential conflicts of interest with respect to the research, authorship, and/or publication of this article.

References

1. Prakash, K.S.; Nancharaih, T.; Rao, V.V.S. Additive Manufacturing Techniques in Manufacturing—An Overview. *Mater. Today Proc.* **2018**, *5*, 3873–3882. [CrossRef]
2. Karakurt, I.; Lin, L. 3D Printing Technologies: Techniques, Materials, and Post-Processing. *Curr. Opin. Chem. Eng.* **2020**, *28*, 134–143. [CrossRef]
3. Cruz Sanchez, F.A.; Boudaoud, H.; Camargo, M.; Pearce, J.M. Plastic Recycling in Additive Manufacturing: A Systematic Literature Review and Opportunities for the Circular Economy. *J. Clean. Prod.* **2020**, *264*, 121602. [CrossRef]
4. Francois, M.M.; Sun, A.; King, W.E.; Henson, N.J.; Tourret, D.; Bronkhorst, C.A.; Carlson, N.N.; Newman, C.K.; Haut, T.; Bakosi, J.; et al. Modeling of Additive Manufacturing Processes for Metals: Challenges and Opportunities. *Curr. Opin. Solid State Mater. Sci.* **2017**, *21*, 198–206. [CrossRef]
5. Pelz, J.S.; Ku, N.; Meyers, M.A.; Vargas-Gonzalez, L.R. Additive Manufacturing of Structural Ceramics: A Historical Perspective. *J. Mater. Res. Technol.* **2021**, *15*, 670–695. [CrossRef]
6. Bove, A.; Calignano, F.; Galati, M.; Iuliano, L. Photopolymerization of Ceramic Resins by Stereolithography Process: A Review. *Appl. Sci.* **2022**, *12*, 3591. [CrossRef]
7. Hull, C.W. Apparatus for Production of Three-Dimensional Objects by Stereolithography. U.S. Patent 638905 8 August 1984.
8. Maas, J.; Liu, B.; Hajela, S.; Huang, Y.; Gong, X.; Chappell, W.J. Laser-Based Layer-by-Layer Polymer Stereolithography for High-Frequency Applications. *Proc. IEEE* **2017**, *105*, 645–654. [CrossRef]
9. Gornet, T. History of Additive Manufacturing. In *3D Printing and Its Impact on the Production of Fully Functional Components: Emerging Research and Opportunities*; IGI Global: Hershey, PA, USA, 2017; pp. 1–24. [CrossRef]
10. Huang, B.; Singamneni, S.B. Curved Layer Adaptive Slicing (CLAS) for Fused Deposition Modelling. *Rapid Prototyp. J.* **2015**, *21*, 354–367. [CrossRef]
11. Samykano, M.; Selvamani, S.K.; Kadirgama, K.; Ngui, W.K.; Kanagaraj, G.; Sudhakar, K. Mechanical Property of FDM Printed ABS: Influence of Printing Parameters. *Int. J. Adv. Manuf. Technol.* **2019**, *102*, 2779–2796. [CrossRef]
12. Lannunziata, E.; Saboori, A.; Galati, M.; Iuliano, L. Laser Powder Bed Fusion of AISI 316L Lattice Structures for Biomedical Applications. *Mater. Today Proc.* **2022**, *70*, 345–351. [CrossRef]
13. Olivas-Alanis, L.H.; Fraga-Martínez, A.A.; García-López, E.; Lopez-Botello, O.; Vazquez-Lepe, E.; Cuan-Urquizo, E.; Rodriguez, C.A. Mechanical Properties of AISI 316L Lattice Structures via Laser Powder Bed Fusion as a Function of Unit Cell Features. *Materials* **2023**, *16*, 1025. [CrossRef] [PubMed]
14. Devarajan, B.; Bhuvaneswari, V.; Arulmurugan, B.; Narayana, A.V.N.S.L.; Priya, A.K.; Abbaraju, V.D.N.K.; Mukunthan, K.S.; Sharma, A.K.; Ting, S.S.; Masi, C. Hybrid Novel Additive Manufacturing for Sustainable Usage of Waste. *J. Nanomater.* **2022**, *2022*, 2697036. [CrossRef]
15. Faludi, J.; Bayley, C.; Bhogal, S.; Iribarne, M. Comparing Environmental Impacts of Additive Manufacturing vs Traditional Machining via Life-Cycle Assessment. *Rapid Prototyp. J.* **2015**, *21*, 14–33. [CrossRef]
16. Von Cieminski, G. *Advances in Production Management Systems*; Springer: Cham, Switzerland, 1983; Volume 4, ISSN 9783319227580.
17. Atzeni, E.; Iuliano, L.; Marchiandi, G.; Minetola, P.; Salmi, A.; Bassoli, E.; Denti, L.; Gatto, A. Additive Manufacturing as a Cost-Effective Way to Produce Metal Parts. In Proceedings of the High Value Manufacturing: Advanced Research in Virtual and Rapid Prototyping-Proceedings of the 6th International Conference on Advanced Research and Rapid Prototyping, VR@ P, Leiria, Portugal, 1–5 October 2013; pp. 3–8.
18. Thomas, D. Costs, Benefits, and Adoption of Additive Manufacturing: A Supply Chain Perspective. *Int. J. Adv. Manuf. Technol.* **2016**, *85*, 1857–1876. [CrossRef] [PubMed]
19. Delic, M.; Eyers, D.R. The Effect of Additive Manufacturing Adoption on Supply Chain Flexibility and Performance: An Empirical Analysis from the Automotive Industry. *Int. J. Prod. Econ.* **2020**, *228*, 107689. [CrossRef]
20. Luomaranta, T.; Martinsuo, M. Supply Chain Innovations for Additive Manufacturing. *Int. J. Phys. Distrib. Logist. Manag.* **2020**, *50*, 54–79. [CrossRef]
21. Attaran, M. Additive Manufacturing: The Most Promising Technology to Alter the Supply Chain and Logistics. *J. Serv. Sci. Manag.* **2017**, *10*, 189–206. [CrossRef]
22. Yadav, A.; Srivastav, A.; Singh, A.; Mushtaque, M.D.; Khan, S.A.; Kumar, H.; Arora, P.K. Investigation on the Materials Used in Additive Manufacturing: A Study. *Mater. Today Proc.* **2020**, *43*, 154–157. [CrossRef]
23. Bhuvanesh Kumar, M.; Sathiya, P. Methods and Materials for Additive Manufacturing: A Critical Review on Advancements and Challenges. *Thin-Walled Struct.* **2021**, *159*, 107228. [CrossRef]
24. Kumbhar, N.N.; Mulay, A.V. Post Processing Methods Used to Improve Surface Finish of Products Which Are Manufactured by Additive Manufacturing Technologies: A Review. *J. Inst. Eng. Ser. C* **2018**, *99*, 481–487. [CrossRef]

25. Cao, L.; Li, J.; Hu, J.; Liu, H.; Wu, Y.; Zhou, Q. Optimization of Surface Roughness and Dimensional Accuracy in LPBF Additive Manufacturing. *Opt. Laser Technol.* **2021**, *142*, 107246. [CrossRef]
26. Brennan, M.C.; Keist, J.S.; Palmer, T.A. Defects in Metal Additive Manufacturing Processes. *J. Mater. Eng. Perform.* **2021**, *30*, 4808–4818. [CrossRef]
27. Hauser, T.; Reisch, R.T.; Breese, P.P.; Lutz, B.S.; Pantano, M.; Nalam, Y.; Bela, K.; Kamps, T.; Volpp, J.; Kaplan, A.F.H. Porosity in Wire Arc Additive Manufacturing of Aluminium Alloys. *Addit. Manuf.* **2021**, *41*, 101993. [CrossRef]
28. Hernandez-Contreras, A.; Ruiz-Huerta, L.; Caballero-Ruiz, A.; Moock, V.; Siller, H.R. Extended CT Void Analysis in FDM Additive Manufacturing Components. *Materials* **2020**, *13*, 3831. [CrossRef] [PubMed]
29. Gui, Y.; Aoyagi, K.; Bian, H.; Chiba, A. Detection, Classification and Prediction of Internal Defects from Surface Morphology Data of Metal Parts Fabricated by Powder Bed Fusion Type Additive Manufacturing Using an Electron Beam. *Addit. Manuf.* **2022**, *54*, 102736. [CrossRef]
30. Raam Kumar, S.; Sridhar, S.; Venkatraman, R.; Venkatesan, M. Polymer Additive Manufacturing of ASA Structure: Influence of Printing Parameters on Mechanical Properties. *Mater. Today Proc.* **2020**, *39*, 1316–1319. [CrossRef]
31. Hu, Q.; Rance, G.A.; Trindade, G.F.; Pervan, D.; Jiang, L.; Foerster, A.; Turyanska, L.; Tuck, C.; Irvine, D.J.; Hague, R.; et al. The Influence of Printing Parameters on Multi-Material Two-Photon Polymerisation Based Micro Additive Manufacturing. *Addit. Manuf.* **2022**, *51*, 102575. [CrossRef]
32. Camposeco-Negrete, C.; Varela-Soriano, J.; Rojas-Carreón, J.J. The Effects of Printing Parameters on Quality, Strength, Mass, and Processing Time of Polylactic Acid Specimens Produced by Additive Manufacturing. *Prog. Addit. Manuf.* **2021**, *6*, 821–840. [CrossRef]
33. Khorasani, M.; Ghasemi, A.H.; Rolfe, B.; Gibson, I. Additive Manufacturing a Powerful Tool for the Aerospace Industry. *Rapid Prototyp. J.* **2022**, *28*, 87–100. [CrossRef]
34. Liu, R.; Wang, Z.; Sparks, T.; Liou, F.; Newkirk, J. *Aerospace Applications of Laser Additive Manufacturing*; Elsevier Ltd.: Amsterdam, The Netherlands, 2017; ISBN 9780081004340.
35. Leal, R.; Barreiros, F.M.; Alves, L.; Romeiro, F.; Vasco, J.C.; Santos, M.; Marto, C. Additive Manufacturing Tooling for the Automotive Industry. *Int. J. Adv. Manuf. Technol.* **2017**, *92*, 1671–1676. [CrossRef]
36. Dwivedi, G.; Srivastava, S.K.; Srivastava, R.K. Analysis of Barriers to Implement Additive Manufacturing Technology in the Indian Automotive Sector. *Int. J. Phys. Distrib. Logist. Manag.* **2017**, *47*, 972–991. [CrossRef]
37. Salifu, S.; Desai, D.; Ogunbiyi, O.; Mwale, K. Recent Development in the Additive Manufacturing of Polymer-Based Composites for Automotive Structures—A Review. *Int. J. Adv. Manuf. Technol.* **2022**, *119*, 6877–6891. [CrossRef]
38. Böckin, D.; Tillman, A.-M. Environmental Assessment of Additive Manufacturing in the Automotive Industry. *J. Clean. Prod.* **2019**, *226*, 977–987. [CrossRef]
39. Vignesh, M.; Ranjith Kumar, G.; Sathishkumar, M.; Manikandan, M.; Rajyalakshmi, G.; Ramanujam, R.; Arivazhagan, N. Development of Biomedical Implants through Additive Manufacturing: A Review. *J. Mater. Eng. Perform.* **2021**, *30*, 4735–4744. [CrossRef]
40. Oliveira, T.T.; Reis, A.C. Fabrication of Dental Implants by the Additive Manufacturing Method: A Systematic Review. *J. Prosthet. Dent.* **2019**, *122*, 270–274. [CrossRef] [PubMed]
41. Sing, S.L.; An, J.; Yeong, W.Y.; Wiria, F.E. Laser and Electron-Beam Powder-Bed Additive Manufacturing of Metallic Implants: A Review on Processes, Materials and Designs. *J. Orthop. Res.* **2016**, *34*, 369–385. [CrossRef]
42. Wang, Y.; Fu, P.; Wang, N.; Peng, L.; Kang, B.; Zeng, H.; Yuan, G.; Ding, W. Challenges and Solutions for the Additive Manufacturing of Biodegradable Magnesium Implants. *Engineering* **2020**, *6*, 1267–1275. [CrossRef]
43. Mohammed, M.I.; Tatineni, J.; Cadd, B.; Peart, G.; Gibson, I. Applications of 3D Topography Scanning and Multi-Material Additive Manufacturing for Facial Prosthesis Development and Production. In Proceedings of the Solid Freeform Fabrication 2016: Proceedings of the 26th Annual International Solid Freeform Fabrication Symposium—An Additive Manufacturing Conference, Austin, TX, USA, 8–10 August 2016; pp. 1695–1707.
44. Coulter, F.B.; Schaffner, M.; Faber, J.A.; Rafsanjani, A.; Smith, R.; Appa, H.; Zilla, P.; Bezuidenhout, D.; Studart, A.R. Bioinspired Heart Valve Prosthesis Made by Silicone Additive Manufacturing. *Matter* **2019**, *1*, 266–279. [CrossRef]
45. Soares, B.; Ribeiro, I.; Cardeal, G.; Leite, M.; Carvalho, H.; Peças, P. Social Life Cycle Performance of Additive Manufacturing in the Healthcare Industry: The Orthosis and Prosthesis Cases. *Int. J. Comput. Integr. Manuf.* **2021**, *34*, 327–340. [CrossRef]
46. *ISO/ASTM 52900*; Standard Terminology for Additive Manufacturing–General Principles–Terminology. International Organization for Standardization: Geneva, Switzerland, 2015.
47. Mazurchevici, A.D.; Nedelcu, D.; Popa, R. Additive Manufacturing of Composite Materials by FDM Technology: A Review. *Indian J. Eng. Mater. Sci.* **2020**, *27*, 179–192. [CrossRef]
48. D'andrea, D.; Risitano, G.; Raffaele, M.; Cucinotta, F.; Santonocito, D. Damage Assessment of Different FDM-Processed Materials Adopting Infrared Thermography. *Frat. Integr. Strutt.* **2022**, *16*, 75–90. [CrossRef]
49. Halloran, J.W. Ceramic Stereolithography: Additive Manufacturing for Ceramics by Photopolymerization. *Annu. Rev. Mater. Res.* **2016**, *46*, 19–40. [CrossRef]
50. Li, H.; Song, L.; Sun, J.; Ma, J.; Shen, Z. Dental Ceramic Prostheses by Stereolithography-Based Additive Manufacturing: Potentials and Challenges. *Adv. Appl. Ceram.* **2019**, *118*, 30–36. [CrossRef]

51. Borlaf, M.; Serra-Capdevila, A.; Colominas, C.; Graule, T. Development of UV-Curable ZrO2 Slurries for Additive Manufacturing (LCM-DLP) Technology. *J. Eur. Ceram. Soc.* **2019**, *39*, 3797–3803. [CrossRef]
52. Wiese, M.; Kwauka, A.; Thiede, S.; Herrmann, C. Economic Assessment for Additive Manufacturing of Automotive End-Use Parts through Digital Light Processing (DLP). *CIRP J. Manuf. Sci. Technol.* **2021**, *35*, 268–280. [CrossRef]
53. D'Andrea, D.; Risitano, G.; Guglielmino, E.; Piperopoulos, E.; Santonocito, D. Correlation between Mechanical Behaviour and Microstructural Features of AISI 316L Produced by SLM. *Procedia Struct. Integr.* **2022**, *41*, 199–207. [CrossRef]
54. Zhang, L.C.; Liu, Y.; Li, S.; Hao, Y. Additive Manufacturing of Titanium Alloys by Electron Beam Melting: A Review. *Adv. Eng. Mater.* **2018**, *20*, 1700842. [CrossRef]
55. Azami, M.; Siahsarani, A.; Hadian, A.; Kazemi, Z.; Rahmatabadi, D.; Kashani-Bozorg, S.F.; Abrinia, K. Laser Powder Bed Fusion of Alumina/Fe–Ni Ceramic Matrix Particulate Composites Impregnated with a Polymeric Resin. *J. Mater. Res. Technol.* **2023**, *24*, 3133–3144. [CrossRef]
56. Saboori, A.; Aversa, A.; Marchese, G.; Biamino, S.; Lombardi, M.; Fino, P. Application of Directed Energy Deposition-Based Additive Manufacturing in Repair. *Appl. Sci.* **2019**, *9*, 3316. [CrossRef]
57. Haley, J.C.; Schoenung, J.M.; Lavernia, E.J. Modelling Particle Impact on the Melt Pool and Wettability Effects in Laser Directed Energy Deposition Additive Manufacturing. *Mater. Sci. Eng. A* **2019**, *761*, 138052. [CrossRef]
58. Gaytan, S.M.; Cadena, M.A.; Karim, H.; Delfin, D.; Lin, Y.; Espalin, D.; MacDonald, E.; Wicker, R.B. Fabrication of Barium Titanate by Binder Jetting Additive Manufacturing Technology. *Ceram. Int.* **2015**, *41*, 6610–6619. [CrossRef]
59. Lores, A.; Azurmendi, N.; Agote, I.; Zuza, E. A Review on Recent Developments in Binder Jetting Metal Additive Manufacturing: Materials and Process Characteristics. *Powder Metall.* **2019**, *62*, 267–296. [CrossRef]
60. Vu, I.Q.; Bass, L.B.; Williams, C.B.; Dillard, D.A. Characterizing the Effect of Print Orientation on Interface Integrity of Multi-Material Jetting Additive Manufacturing. *Addit. Manuf.* **2018**, *22*, 447–461. [CrossRef]
61. Sturm, L.D.; Albakri, M.I.; Tarazaga, P.A.; Williams, C.B. In Situ Monitoring of Material Jetting Additive Manufacturing Process via Impedance Based Measurements. *Addit. Manuf.* **2019**, *28*, 456–463. [CrossRef]
62. Ghajari, A. Sheet Lamination Additive Manufacturing of 316L/AISI 4140 Parts Using Friction Stir Method. **2023**. *preprint*. [CrossRef]
63. Bhatt, P.M.; Kabir, A.M.; Peralta, M.; Bruck, H.A.; Gupta, S.K. A Robotic Cell for Performing Sheet Lamination-Based Additive Manufacturing. *Addit. Manuf.* **2019**, *27*, 278–289. [CrossRef]
64. Bedmar, J.; Riquelme, A.; Rodrigo, P.; Torres, B.; Rams, J. Comparison of Different Additive Manufacturing Methods for 316l Stainless Steel. *Materials* **2021**, *14*, 6504. [CrossRef]
65. Avanzini, A. Fatigue Behavior of Additively Manufactured Stainless Steel 316L. *Materials* **2023**, *16*, 65. [CrossRef]
66. Kasha, A.; Obadimu, S.O.; Kourousis, K.I. Flexural Characteristics of Material Extrusion Steel 316L: Influence of Manufacturing Parameters. *Addit. Manuf. Lett.* **2022**, *3*, 100087. [CrossRef]
67. Aversa, A.; Saboori, A.; Librera, E.; de Chirico, M.; Biamino, S.; Lombardi, M.; Fino, P. The Role of Directed Energy Deposition Atmosphere Mode on the Microstructure and Mechanical Properties of 316L Samples. *Addit. Manuf.* **2020**, *34*, 101274. [CrossRef]
68. Kale, A.B.; Kim, B.K.; Kim, D.I.; Castle, E.G.; Reece, M.; Choi, S.H. An Investigation of the Corrosion Behavior of 316L Stainless Steel Fabricated by SLM and SPS Techniques. *Mater. Charact.* **2020**, *163*, 110204. [CrossRef]
69. Nguyen, D.; Park, H.; Lee, C. Applying Selective Laser Melting to Join Al and Fe: An Investigation of Dissimilar Materials. *Appl. Sci.* **2019**, *9*, 3031. [CrossRef]
70. Dzogbewu, T.C.; du Preez, W.B. Additive Manufacturing of Ti-Based Intermetallic Alloys: A Review and Conceptualization of a next-Generation Machine. *Materials* **2021**, *14*, 4317. [CrossRef]
71. Gokuldoss, P.K. *Selective Laser Melting: Materials and Applications*; MDPI: Basel, Switzerland, 2020; ISSN 3039285785.
72. Yadroitsev, I.; Yadroitsava, I.; Du Plessis, A.; MacDonald, E. *Fundamentals of Laser Powder Bed Fusion of Metals*; Elsevier: Amsterdam, The Netherlands, 2021; ISBN 0128240911.
73. Yadroitsev, I.; Yadroitsava, I.; Du Plessis, A. Basics of Laser Powder Bed Fusion. In *Fundamentals of Laser Powder Bed Fusion of Metals*; Elsevier: Amsterdam, The Netherlands, 2021; pp. 15–38.
74. Suryawanshi, J.; Prashanth, K.G.; Ramamurty, U. Mechanical Behavior of Selective Laser Melted 316L Stainless Steel. *Mater. Sci. Eng. A* **2017**, *696*, 113–121. [CrossRef]
75. Siri, C.; Popa, I.; Vion, A.; Langlade, C.; Chevalier, S. Impact of Selective Laser Melting Additive Manufacturing on the High Temperature Behavior of AISI 316L Austenitic Stainless Steel. *Oxid. Met.* **2020**, *94*, 527–548. [CrossRef]
76. Rosa, F.; Manzoni, S.; Casati, R. Damping Behavior of 316L Lattice Structures Produced by Selective Laser Melting. *Mater. Des.* **2018**, *160*, 1010–1018. [CrossRef]
77. Vastola, G.; Zhang, G.; Pei, Q.X.; Zhang, Y.W. Modeling and Control of Remelting in High-Energy Beam Additive Manufacturing. *Addit. Manuf.* **2015**, *7*, 57–63. [CrossRef]
78. Astafurova, E.G.; Panchenko, M.Y.; Moskvina, V.A.; Maier, G.G.; Astafurov, S.V.; Melnikov, E.V.; Fortuna, A.S.; Reunova, K.A.; Rubtsov, V.E.; Kolubaev, E.A. Microstructure and Grain Growth Inhomogeneity in Austenitic Steel Produced by Wire-Feed Electron Beam Melting: The Effect of Post-Building Solid-Solution Treatment. *J. Mater. Sci.* **2020**, *55*, 9211–9224. [CrossRef]
79. Wang, C.; Tan, X.; Liu, E.; Tor, S.B. Process Parameter Optimization and Mechanical Properties for Additively Manufactured Stainless Steel 316L Parts by Selective Electron Beam Melting. *Mater. Des.* **2018**, *147*, 157–166. [CrossRef]

80. Yadollahi, A.; Shamsaei, N.; Thompson, S.M.; Seely, D.W. Effects of Process Time Interval and Heat Treatment on the Mechanical and Microstructural Properties of Direct Laser Deposited 316L Stainless Steel. *Mater. Sci. Eng. A* **2015**, *644*, 171–183. [CrossRef]
81. Guo, P.; Zou, B.; Huang, C.; Gao, H. Study on Microstructure, Mechanical Properties and Machinability of Efficiently Additive Manufactured AISI 316L Stainless Steel by High-Power Direct Laser Deposition. *J. Mater. Process. Technol.* **2017**, *240*, 12–22. [CrossRef]
82. Saboori, A.; Aversa, A.; Marchese, G.; Biamino, S.; Lombardi, M.; Fino, P. Microstructure and Mechanical Properties of AISI 316L Produced by Directed Energy Deposition-Based Additive Manufacturing: A Review. *Appl. Sci.* **2020**, *10*, 3310. [CrossRef]
83. Moheimani, S.K.; Iuliano, L.; Saboori, A. The Role of Substrate Preheating on the Microstructure, Roughness, and Mechanical Performance of AISI 316L Produced by Directed Energy Deposition Additive Manufacturing. *Int. J. Adv. Manuf. Technol.* **2022**, *119*, 7159–7174. [CrossRef]
84. Azinpour, E.; Darabi, R.; Cesar de Sa, J.; Santos, A.; Hodek, J.; Dzugan, J. Fracture Analysis in Directed Energy Deposition (DED) Manufactured 316L Stainless Steel Using a Phase-Field Approach. *Finite Elem. Anal. Des.* **2020**, *177*, 103417. [CrossRef]
85. Xu, K.; Li, B.; Jiang, C. Adjusting Microstructure and Improving Mechanical Property of Additive Manufacturing 316L Based on Process Optimization. *Mater. Sci. Eng. A* **2023**, *870*, 144824. [CrossRef]
86. Mirzababaei, S.; Pasebani, S. A Review on Binder Jet Additive Manufacturing of 316L Stainless Steel. *J. Manuf. Mater. Process.* **2019**, *3*, 8–12. [CrossRef]
87. Meenashisundaram, G.K.; Xu, Z.; Nai, M.L.S.; Lu, S.; Ten, J.S.; Wei, J. Binder Jetting Additive Manufacturing of High Porosity 316L Stainless Steel Metal Foams. *Materials* **2020**, *13*, 3744. [CrossRef]
88. Atapour, M.; Wang, X.; Persson, M.; Odnevall Wallinder, I.; Hedberg, Y.S. Corrosion of Binder Jetting Additively Manufactured 316L Stainless Steel of Different Surface Finish. *J. Electrochem. Soc.* **2020**, *167*, 131503. [CrossRef]
89. Lecis, N.; Mariani, M.; Beltrami, R.; Emanuelli, L.; Casati, R.; Vedani, M.; Molinari, A. Effects of Process Parameters, Debinding and Sintering on the Microstructure of 316L Stainless Steel Produced by Binder Jetting. *Mater. Sci. Eng. A* **2021**, *828*, 142108. [CrossRef]
90. Cai, J.; Zhang, B.; Qu, X. Microstructure Evolution and Mechanical Behavior of SS316L Alloy Fabricated by a Non-Toxic and Low Residue Binder Jetting Process. *Appl. Surf. Sci.* **2023**, *616*, 156589. [CrossRef]
91. Sadaf, M.; Bragaglia, M.; Nanni, F. A Simple Route for Additive Manufacturing of 316L Stainless Steel via Fused Filament Fabrication. *J. Manuf. Process.* **2021**, *67*, 141–150. [CrossRef]
92. Carminati, M.; Quarto, M.; D'urso, G.; Giardini, C.; Borriello, C. A Comprehensive Analysis of AISI 316L Samples Printed via FDM: Structural and Mechanical Characterization. *Key Eng. Mater.* **2022**, *926*, 46–55. [CrossRef]
93. Carminati, M.; Quarto, M.; D'urso, G.; Giardini, C.; Maccarini, G. Mechanical Characterization of AISI 316L Samples Printed Using Material Extrusion. *Appl. Sci.* **2022**, *12*, 1433. [CrossRef]
94. Quarto, M.; Carminati, M.; D'Urso, G. Density and Shrinkage Evaluation of AISI 316L Parts Printed via FDM Process. *Mater. Manuf. Process.* **2021**, *36*, 1535–1543. [CrossRef]
95. Sampedro, G.A.R.; Rachmawati, S.M.; Kim, D.S.; Lee, J.M. Exploring Machine Learning-Based Fault Monitoring for Polymer-Based Additive Manufacturing: Challenges and Opportunities. *Sensors* **2022**, *22*, 9446. [CrossRef] [PubMed]
96. Vinoth, V.; Sathiyamurthy, S.; Natarajan, U.; Venkatkumar, D.; Prabhakaran, J.; Sanjeevi Prakash, K. Examination of Microstructure Properties of AISI 316L Stainless Steel Fabricated by Wire Arc Additive Manufacturing. *Mater. Today Proc.* **2022**, *66*, 702–706. [CrossRef]
97. Ivántabernero; Paskual, A.; Álvarez, P.; Suárez, A. Study on Arc Welding Processes for High Deposition Rate Additive Manufacturing. *Procedia CIRP* **2018**, *68*, 358–362. [CrossRef]
98. Sowrirajan, M.; Vijayananthan, M.; Seenivasagan, G.; Sundaresan, J. A New Approach to the Fabrication of Thin-Walled Plate Component through Typical Wire Arc Additive Manufacturing. *J. Adv. Mech. Sci.* **2022**, *1*, 8–13. [CrossRef]
99. Rodrigues, T.A.; Cipriano Farias, F.W.; Zhang, K.; Shamsolhodaei, A.; Shen, J.; Zhou, N.; Schell, N.; Capek, J.; Polatidis, E.; Santos, T.G.; et al. Wire and Arc Additive Manufacturing of 316L Stainless Steel/Inconel 625 Functionally Graded Material: Development and Characterization. *J. Mater. Res. Technol.* **2022**, *21*, 237–251. [CrossRef]
100. Ozsoy, A.; Tureyen, E.B.; Baskan, M.; Yasa, E. Microstructure and Mechanical Properties of Hybrid Additive Manufactured Dissimilar 17-4 PH and 316L Stainless Steels. *Mater. Today Commun.* **2021**, *28*, 102561. [CrossRef]
101. Hietala, M.; Rautio, T.; Makikangas, J.; Jaskari, M.; Keskitalo, M.; Jarvenpaa, A. Static Properties and Fatigue Strength of Wire Arc Additive Manufactured 316L. In Proceedings of the 2022 7th National Scientific Conference on Applying New Technology in Green Buildings (ATiGB), Da Nang, Vietnam, 11–12 November 2022; pp. 1–5. [CrossRef]
102. Zhang, K.; Wang, S.; Liu, W.; Shang, X. Characterization of Stainless Steel Parts by Laser Metal Deposition Shaping. *Mater. Des.* **2014**, *55*, 104–119. [CrossRef]
103. Zhong, Y.; Rännar, L.E.; Liu, L.; Koptyug, A.; Wikman, S.; Olsen, J.; Cui, D.; Shen, Z. Additive Manufacturing of 316L Stainless Steel by Electron Beam Melting for Nuclear Fusion Applications. *J. Nuclear Mater.* **2017**, *486*, 234–245. [CrossRef]
104. Nastac, M.; Klein, R.L.A. Microstructure and Mechanical Properties Comparison of 316L Parts Produced by Different Additive Manufacturing Processes. In Proceedings of the Solid Freeform Fabrication 2017: Proceedings of the 28th Annual International Solid Freeform Fabrication Symposium—An Additive Manufacturing Conference, Austin, TX, USA, 7–9 August 2017; pp. 332–341.

105. Kim, F.H.; Moylan, S.P. *Literature Review of Metal Additive Manufacturing Defects*; NIST Advanced Manufacturing Series; US Department of Commerce, National Institute of Standards and Technology: Gaithersburg, MD, USA, 2018; pp. 1–17.
106. Stern, F.; Tenkamp, J.; Walther, F. Non-Destructive Characterization of Process-Induced Defects and Their Effect on the Fatigue Behavior of Austenitic Steel 316L Made by Laser-Powder Bed Fusion. *Prog. Addit. Manuf.* **2020**, *5*, 287–294. [CrossRef]
107. Bartlett, J.L.; Jarama, A.; Jones, J.; Li, X. Prediction of Microstructural Defects in Additive Manufacturing from Powder Bed Quality Using Digital Image Correlation. *Mater. Sci. Eng. A* **2020**, *794*, 140002. [CrossRef]
108. Snow, Z.; Scime, L.; Ziabari, A.; Fisher, B.; Paquit, V. Observation of Spatter-Induced Stochastic Lack-of-Fusion in Laser Powder Bed Fusion Using in Situ Process Monitoring. *Addit. Manuf.* **2023**, *61*, 103298. [CrossRef]
109. Zhang, B.; Li, Y.; Bai, Q. Defect Formation Mechanisms in Selective Laser Melting: A Review. *Chin. J. Mech. Eng. (Engl. Ed.)* **2017**, *30*, 515–527. [CrossRef]
110. Santonocito, D.; Fintová, S.; Di Cocco, V.; Iacoviello, F.; Risitano, G.; D'Andrea, D. Comparison on Mechanical Behaviour and Microstructural Features Between Traditional and AM AISI 316L. *Fatigue Fract. Eng. Mater. Struct.* **2023**, *46*, 379–395. [CrossRef]
111. Mukherjee, T.; DebRoy, T. Mitigation of Lack of Fusion Defects in Powder Bed Fusion Additive Manufacturing. *J. Manuf. Process.* **2018**, *36*, 442–449. [CrossRef]
112. Khairallah, S.A.; Anderson, A.T.; Rubenchik, A.; King, W.E. Laser Powder-Bed Fusion Additive Manufacturing: Physics of Complex Melt Flow and Formation Mechanisms of Pores, Spatter, and Denudation Zones. *Acta Mater.* **2016**, *108*, 36–45. [CrossRef]
113. DebRoy, T.; Wei, H.L.; Zuback, J.S.; Mukherjee, T.; Elmer, J.W.; Milewski, J.O.; Beese, A.M.; Wilson-Heid, A.; De, A.; Zhang, W. Additive Manufacturing of Metallic Components—Process, Structure and Properties. *Prog. Mater. Sci.* **2018**, *92*, 112–224. [CrossRef]
114. King, W.E.; Barth, H.D.; Castillo, V.M.; Gallegos, G.F.; Gibbs, J.W.; Hahn, D.E.; Kamath, C.; Rubenchik, A.M. Observation of Keyhole-Mode Laser Melting in Laser Powder-Bed Fusion Additive Manufacturing. *J. Mater. Process. Technol.* **2014**, *214*, 2915–2925. [CrossRef]
115. Martin, A.A.; Calta, N.P.; Khairallah, S.A.; Wang, J.; Depond, P.J.; Fong, A.Y.; Thampy, V.; Guss, G.M.; Kiss, A.M.; Stone, K.H.; et al. Dynamics of Pore Formation during Laser Powder Bed Fusion Additive Manufacturing. *Nat. Commun.* **2019**, *10*, 1987. [CrossRef] [PubMed]
116. Wang, L.; Zhao, Y.; Li, Y.; Zhan, X. Droplet Transfer Induced Keyhole Fluctuation and Its Influence Regulation on Porosity Rate during Hybrid Laser Arc Welding of Aluminum Alloys. *Metals* **2021**, *11*, 1510. [CrossRef]
117. Rabin, B.H.; Smolik, G.R.; Korth, G.E. Characterization of Entrapped Gases in Rapidly Solidified Powders. *Mater. Sci. Eng. A* **1990**, *124*, 1–7. [CrossRef]
118. Elmer, J.W.; Vaja, J.; Carlton, H.D.; Pong, R. The Effect of Ar and N2 Shielding Gas on Laser Weld Porosity in Steel, Stainless Steels, and Nickel. *Weld. J.* **2015**, *94*, 313s–325s.
119. Kaynak, Y.; Kitay, O. Porosity, Surface Quality, Microhardness and Microstructure of Selective Laser Melted 316l Stainless Steel Resulting from Finish Machining. *J. Manuf. Mater. Process.* **2018**, *2*, 36. [CrossRef]
120. Slotwinski, J.A.; Garboczi, E.J.; Hebenstreit, K.M. Porosity Measurements and Analysis for Metal Additive Manufacturing Process Control. *J. Res. Natl. Inst. Stand. Technol.* **2014**, *119*, 494–528. [CrossRef]
121. Ziółkowski, G.; Chlebus, E.; Szymczyk, P.; Kurzac, J. Application of X-Ray CT Method for Discontinuity and Porosity Detection in 316L Stainless Steel Parts Produced with SLM Technology. *Arch. Civ. Mech. Eng.* **2014**, *14*, 608–614. [CrossRef]
122. Jaskari, M.; Mäkikangas, J.; Järvenpää, A.; Mäntyjärvi, K.; Karjalainen, P. Effect of High Porosity on Bending Fatigue Properties of 3D Printed AISI 316L Steel. *Procedia Manuf.* **2019**, *36*, 33–41. [CrossRef]
123. Karakaş, Ö.; Kardeş, F.B.; Foti, P.; Berto, F. An Overview of Factors Affecting High-Cycle Fatigue of Additive Manufacturing Metals. *Fatigue Fract. Eng. Mater. Struct.* **2023**, *46*, 1649–1668. [CrossRef]
124. Solberg, K.; Guan, S.; Razavi, S.M.J.; Welo, T.; Chan, K.C.; Berto, F. Fatigue of Additively Manufactured 316L Stainless Steel: The Influence of Porosity and Surface Roughness. *Fatigue Fract. Eng. Mater. Struct.* **2019**, *42*, 2043–2052. [CrossRef]
125. Mercelis, P.; Kruth, J.P. Residual Stresses in Selective Laser Sintering and Selective Laser Melting. *Rapid Prototyp. J.* **2006**, *12*, 254–265. [CrossRef]
126. Chen, S.; Gao, H.; Zhang, Y.; Wu, Q.; Gao, Z.; Zhou, X. Review on Residual Stresses in Metal Additive Manufacturing: Formation Mechanisms, Parameter Dependencies, Prediction and Control Approaches. *J. Mater. Res. Technol.* **2022**, *17*, 2950–2974. [CrossRef]
127. Simson, T.; Emmel, A.; Dwars, A.; Böhm, J. Residual Stress Measurements on AISI 316L Samples Manufactured by Selective Laser Melting. *Addit. Manuf.* **2017**, *17*, 183–189. [CrossRef]
128. Wang, Q.; Zhang, S.; Zhang, C.H.; Wu, C.; Wang, J.; Chen, J.; Sun, Z. Microstructure Evolution and EBSD Analysis of a Graded Steel Fabricated by Laser Additive Manufacturing. *Vacuum* **2017**, *141*, 68–81. [CrossRef]
129. Sander, G.; Babu, A.P.; Gao, X.; Jiang, D.; Birbilis, N. On the Effect of Build Orientation and Residual Stress on the Corrosion of 316L Stainless Steel Prepared by Selective Laser Melting. *Corros. Sci.* **2021**, *179*, 109149. [CrossRef]
130. Barroqueiro, B.; Andrade-Campos, A.; Valente, R.A.F.; Neto, V. Metal Additive Manufacturing Cycle in Aerospace Industry: A Comprehensive Review. *J. Manuf. Mater. Process.* **2019**, *3*, 52. [CrossRef]
131. Hajnys, J.; Pagáč, M.; Měsíček, J.; Petru, J.; Król, M. Influence of Scanning Strategy Parameters on Residual Stress in the SLM Process According to the Bridge Curvature Method for AISI 316L Stainless Steel. *Materials* **2020**, *13*, 1659. [CrossRef]
132. Vinoth Jebaraj, A.; Sugavaneswaran, M. Influence of Shot Peening on Residual Stress Distribution and Corrosion Resistance of Additive Manufactured Stainless Steel AISI 316L. *Trans. Indian Inst. Met.* **2019**, *72*, 1651–1653. [CrossRef]

133. Castro, H.F.; Carvalho, A.R.F.; Leal, F.; Gouveia, H. *Assessing Industry 4.0 Readiness of Portuguese Companies*; Springer: Berlin/Heidelberg, Germany, 2020; ISBN 9783030290405.
134. Khalid, M.; Peng, Q. Investigation of Printing Parameters of Additive Manufacturing Process for Sustainability Using Design of Experiments. *J. Mech. Des.* **2021**, *143*, 32001. [CrossRef]
135. Ingrassia, T.; Nigrelli, V.; Ricotta, V.; Tartamella, C. Process Parameters Influence in Additive Manufacturing. In Proceedings of the Advances on Mechanics, Design Engineering and Manufacturing: Proceedings of the International Joint Conference on Mechanics, Design Engineering & Advanced Manufacturing (JCM 2016), Catania, Italy, 14–16 September 2016; pp. 261–270. [CrossRef]
136. Ahmadi, M.; Tabary, S.A.A.B.; Rahmatabadi, D.; Ebrahimi, M.S.; Abrinia, K.; Hashemi, R. Review of Selective Laser Melting of Magnesium Alloys: Advantages, Microstructure and Mechanical Characterizations, Defects, Challenges, and Applications. *J. Mater. Res. Technol.* **2022**, *19*, 1537–1562. [CrossRef]
137. Fongsamootr, T.; Thawon, I.; Tippayawong, N.; Tippayawong, K.Y.; Suttakul, P. Effect of Print Parameters on Additive Manufacturing of Metallic Parts: Performance and Sustainability Aspects. *Sci. Rep.* **2022**, *12*, 19292. [CrossRef] [PubMed]
138. Zhao, L.; Santos Macías, J.G.; Dolimont, A.; Simar, A.; Rivière-Lorphèvre, E. Comparison of Residual Stresses Obtained by the Crack Compliance Method for Parts Produced by Different Metal Additive Manufacturing Techniques and after Friction Stir Processing. *Addit. Manuf.* **2020**, *36*, 101499. [CrossRef]
139. Mostafaei, A.; Zhao, C.; He, Y.; Reza Ghiaasiaan, S.; Shi, B.; Shao, S.; Shamsaei, N.; Wu, Z.; Kouraytem, N.; Sun, T.; et al. Defects and Anomalies in Powder Bed Fusion Metal Additive Manufacturing. *Curr. Opin. Solid State Mater. Sci.* **2022**, *26*, 100974. [CrossRef]
140. Hinojos, A.; Mireles, J.; Reichardt, A.; Frigola, P.; Hosemann, P.; Murr, L.E.; Wicker, R.B. Joining of Inconel 718 and 316 Stainless Steel Using Electron Beam Melting Additive Manufacturing Technology. *Mater. Des.* **2016**, *94*, 17–27. [CrossRef]
141. Kruth, J.P.; Deckers, J.; Yasa, E.; Wauthlé, R. Assessing and Comparing Influencing Factors of Residual Stresses in Selective Laser Melting Using a Novel Analysis Method. *Proc. Inst. Mech. Eng. Part B J. Eng. Manuf.* **2012**, *226*, 980–991. [CrossRef]
142. Röttger, A.; Geenen, K.; Windmann, M.; Binner, F.; Theisen, W. Comparison of Microstructure and Mechanical Properties of 316 L Austenitic Steel Processed by Selective Laser Melting with Hot-Isostatic Pressed and Cast Material. *Mater. Sci. Eng. A* **2016**, *678*, 365–376. [CrossRef]
143. Do, T.; Bauder, T.J.; Suen, H.; Rego, K.; Yeom, J.; Kwon, P. Additively Manufactured Full-Density Stainless Steel 316L with Binder Jet Printing. In Proceedings of the ASME 2018 13th International Manufacturing Science and Engineering Conference, College Station, TX, USA, 18–22 June 2018; American Society of Mechanical Engineers; Volume 51357, p. V001T01A017.
144. D'Andrea, D.; Gatto, A.; Guglielmino, E.; Risitano, G.; Santonocito, D. A Comparison on Static and Fatigue Behaviour between Traditional and SLM AISI 316L. *J. Mech. Sci. Technol.* **2022**, *37*, 1083–1088. [CrossRef]
145. Britt, C.; Montgomery, C.J.; Brand, M.J.; Liu, Z.K.; Carpenter, J.S.; Beese, A.M. Effect of Processing Parameters and Strut Dimensions on the Microstructures and Hardness of Stainless Steel 316L Lattice-Emulating Structures Made by Powder Bed Fusion. *Addit. Manuf.* **2021**, *40*, 101943. [CrossRef]
146. Bartolomeu, F.; Buciumeanu, M.; Pinto, E.; Alves, N.; Carvalho, O.; Silva, F.S.; Miranda, G. 316L Stainless Steel Mechanical and Tribological Behavior—A Comparison between Selective Laser Melting, Hot Pressing and Conventional Casting. *Addit. Manuf.* **2017**, *16*, 81–89. [CrossRef]
147. Sun, Y.; Moroz, A.; Alrbaey, K. Sliding Wear Characteristics and Corrosion Behaviour of Selective Laser Melted 316L Stainless Steel. *J. Mater. Eng. Perform.* **2014**, *23*, 518–526. [CrossRef]
148. Matthews, M.J.; Guss, G.; Khairallah, S.A.; Rubenchik, A.M.; Depond, P.J.; King, W.E. Denudation of Metal Powder Layers in Laser Powder Bed Fusion Processes. *Acta Mater.* **2016**, *114*, 33–42. [CrossRef]
149. Guo, Q.; Zhao, C.; Escano, L.I.; Young, Z.; Xiong, L.; Fezzaa, K.; Everhart, W.; Brown, B.; Sun, T.; Chen, L. Transient Dynamics of Powder Spattering in Laser Powder Bed Fusion Additive Manufacturing Process Revealed by In-Situ High-Speed High-Energy x-Ray Imaging. *Acta Mater.* **2018**, *151*, 169–180. [CrossRef]
150. Bassis, M.; Kotliar, A.; Koltiar, R.; Ron, T.; Leon, A.; Shirizly, A.; Aghion, E. The Effect of a Slow Strain Rate on the Stress Corrosion Resistance of Austenitic Stainless Steel Produced by the Wire Laser Additive Manufacturing Process. *Metals* **2021**, *11*, 1930. [CrossRef]
151. Bae, K.; Shin, D.; Lee, J.; Kim, S.; Lee, W.; Jo, I.; Lee, J. Corrosion Resistance of Laser Powder Bed Fused AISI 316L Stainless Steel and Effect of Direct Annealing. *Materials* **2022**, *15*, 6336. [CrossRef]
152. Ma, M.; Wang, Z.; Wang, D.; Zeng, X. Control of Shape and Performance for Direct Laser Fabrication of Precision Large-Scale Metal Parts with 316L Stainless Steel. *Opt. Laser Technol.* **2013**, *45*, 209–216. [CrossRef]
153. Guan, K.; Wang, Z.; Gao, M.; Li, X.; Zeng, X. Effects of Processing Parameters on Tensile Properties of Selective Laser Melted 304 Stainless Steel. *Mater. Des.* **2013**, *50*, 581–586. [CrossRef]
154. Tolosa, I.; Garciandía, F.; Zubiri, F.; Zapirain, F.; Esnaola, A. Study of Mechanical Properties of AISI 316 Stainless Steel Processed by "Selective Laser Melting", Following Different Manufacturing Strategies. *Int. J. Adv. Manuf. Technol.* **2010**, *51*, 639–647. [CrossRef]
155. Werner, T.; Madia, M.; Zerbst, U. Comparison of the Fatigue Behavior of Wrought and Additively Manufactured AISI 316L. *Procedia Struct. Integr.* **2021**, *38*, 554–563. [CrossRef]

156. Ponticelli, G.S.; Panciroli, R.; Venettacci, S.; Tagliaferri, F.; Guarino, S. Experimental Investigation on the Fatigue Behavior of Laser Powder Bed Fused 316L Stainless Steel. *CIRP J. Manuf. Sci. Technol.* **2022**, *38*, 787–800. [CrossRef]
157. Blinn, B.; Klein, M.; Gläßner, C.; Smaga, M.; Aurich, J.C.; Beck, T. An Investigation of the Microstructure and Fatigue Behavior of Additively Manufactured AISI 316L Stainless Steel with Regard to the Influence of Heat Treatment. *Metals* **2018**, *8*, 220. [CrossRef]
158. Santonocito, D.; Gatto, A.; Risitano, G. Energy Release as a Parameter for Fatigue Design of Additive Manufactured Metals. *Mater. Des. Process. Commun.* **2021**, *3*, e255. [CrossRef]
159. Kerner, Z.; Horváth, Á.; Nagy, G. Comparative Electrochemical Study of 08H18N10T, AISI 304 and AISI 316L Stainless Steels. *Electrochim. Acta* **2007**, *52*, 7529–7537. [CrossRef]
160. La Barbera, A.; Mignone, A.; Tosto, S.; Vignaud, C. Electron Beam Cladding and Alloying of AISI 316 on Plain Carbon Steel: Microstructure and Electrochemical Corrosion Behaviour. *Surf. Coatings Technol.* **1991**, *46*, 317–329. [CrossRef]
161. Li, Q.; Shen, Y.; Han, P. Serrated Flow Behavior of Aisi 316l Austenitic Stainless Steel for Nuclear Reactors. *IOP Conf. Ser. Mater. Sci. Eng.* **2017**, *250*, 012013. [CrossRef]
162. Jafarpour, S.M.; Puth, A.; Dalke, A.; Böcker, J.; Pipa, A.V.; Röpcke, J.; van Helden, J.P.H.; Biermann, H. Solid Carbon Active Screen Plasma Nitrocarburizing of AISI 316L Stainless Steel in Cold Wall Reactor: Influence of Plasma Conditions. *J. Mater. Res. Technol.* **2020**, *9*, 9195–9205. [CrossRef]
163. de Abreu Mendonça Schvartzman, M.M.; Quinan, M.A.D.; da Costa Campos, W.R.; Lima, L.I.L. Stress Corrosion Cracking of the Aisi 316l Stainless Steel Haz in a Pwr Nuclear Reactor Environment. *Weld. Int.* **2011**, *25*, 15–23. [CrossRef]
164. Chen, C.J.; Wang, M.C.; Wang, D.S.; Liang, H.S.; Feng, P. Characterisations of Electrospark Deposition Stellite 6 Alloy Coating on 316L Sealed Valve Used in Nuclear Power Plant. *Mater. Sci. Technol.* **2010**, *26*, 276–280. [CrossRef]
165. Banerjee, A.; Ntovas, M.; Da Silva, L.; Rahimi, S. Microstructure and Mechanical Properties of Dissimilar Inertia Friction Welded 316L Stainless Steel to A516 Ferritic Steel for Potential Applications in Nuclear Reactors. *Manuf. Lett.* **2022**, *33*, 33–37. [CrossRef]
166. Muthu, S.M.; Mohana Bharathi, C.; Vishal Gukhan, N.; Vignesh Kumar, S.; Venkatesh Kannan, M.; Arivarasu, M.; Manikandan, M.; Arivazhagan, N. Hot Corrosion Studies on Dissimilar Weldments C-22 and AISI 316L in the Molten Salt K_2SO_4 + 60%wt NaCl Environment. *Mater. Today Proc.* **2018**, *5*, 13340–13346. [CrossRef]
167. Ghosh, N.; Kumar Pal, P.; Nandi, G.; Rudrapati, R. Parametric Optimization of Gas Metal Arc Welding Process by PCA Based Taguchi Method on Austenitic Stainless Steel AISI 316L. *Mater. Today Proc.* **2018**, *5*, 1620–1625. [CrossRef]
168. Abass, M.H.; Alali, M.S.; Abbas, W.S.; Shehab, A.A. Study of Solidification Behaviour and Mechanical Properties of Arc Stud Welded AISI 316L Stainless Steel. *J. Achiev. Mater. Manuf. Eng.* **2019**, *97*, 5–14. [CrossRef]
169. Sánchez-Tovar, R.; Montañés, M.T.; García-Antón, J. Effects of Microplasma Arc AISI 316L Welds on the Corrosion Behaviour of Pipelines in LiBr Cooling Systems. *Corros. Sci.* **2013**, *73*, 365–374. [CrossRef]
170. Kožuh, S.; Gojić, L.V.; Ivković, B. Corrosion failure and microstructure analysis of AISI 316L stainless steels for ship pipeline before and after welding. *Kovove Mater.* **2013**, *51*, 53–61. [CrossRef]
171. Tang, J.; Liu, M.; Huang, Y.; Liu, G.; Zang, J.; Liu, S. Effect of Manufacturing Deviations on the Thermohydraulic Performance of Printed Circuit Heat Exchangers with Zigzag Channels. *Appl. Therm. Eng.* **2023**, *219*, 119496. [CrossRef]
172. Solano, J.P.; Martínez, D.S.; Vicente, P.G.; Viedma, A. Enhanced Thermal-Hydraulic Performance in Tubes of Reciprocating Scraped Surface Heat Exchangers. *Appl. Therm. Eng.* **2023**, *220*, 119667. [CrossRef]
173. da Silva, R.P.P.; Mortean, M.V.V.; de Paiva, K.V.; Beckedorff, L.E.; Oliveira, J.L.G.; Brandão, F.G.; Monteiro, A.S.; Carvalho, C.S.; Oliveira, H.R.; Borges, D.G.; et al. Thermal and Hydrodynamic Analysis of a Compact Heat Exchanger Produced by Additive Manufacturing. *Appl. Therm. Eng.* **2021**, *193*, 116973. [CrossRef]
174. Petrescu, D.; Nitu, A.; Golgovici, F.; Demetrescu, I.; Corban, M. Behaviour Aspects of an EB-PVD Alumina (Al_2O_3) Film with an Interlayer (NiCrAlY) Deposited on AISI 316L Steel Investigated in Liquid Lead. *Metals* **2023**, *13*, 616. [CrossRef]
175. Benes, L.; Mouralova, K.; Midula, P.; Snow, J.; Lysonkova, I.; Pilnaj, D.; Burdova, H.; Prokes, T.; Zahradnicek, R.; Fries, J.; et al. The Corrosion Behavior of WEDM Machined Stainless Steels in a Pyrolysis Environment. *Metals* **2023**, *13*, 144. [CrossRef]
176. Silva, C.C.; Farias, J.P.; de Sant'Ana, H.B. Evaluation of AISI 316L Stainless Steel Welded Plates in Heavy Petroleum Environment. *Mater. Des.* **2009**, *30*, 1581–1587. [CrossRef]
177. Zaffora, A.; Di Franco, F.; Santamaria, M. ScienceDirect Electrochemistry Corrosion of Stainless Steel in Food and Pharmaceutical Industry. *Curr. Opin. Electrochem.* **2021**, *29*, 100760. [CrossRef]
178. Le Gentil, C.; Sylla, Y.; Faille, C. Bacterial Re-Contamination of Surfaces of Food Processing Lines during Cleaning in Place Procedures. *J. Food Eng.* **2010**, *96*, 37–42. [CrossRef]
179. Gaylarde, C.C. Comparison of Sodium Hypochlorite and Peracetic Acid as Sanitising Agents for Stainless Steel Food Processing Surfaces Using Epifluorescence Microscopy. *Int. J. Food Microbiol.* **2000**, *61*, 81–85.
180. Tiwari, S.K.; Mishra, T.; Gunjan, M.K.; Bhattacharyya, A.S.; Singh, T.B.; Singh, R. Development and Characterization of Sol—Gel Silica—Alumina Composite Coatings on AISI 316L for Implant Applications. *Surf. Coat. Technol.* **2007**, *201*, 7582–7588. [CrossRef]
181. Hryniewicz, T.; Rokosz, K.; Filippi, M. Biomaterial Studies on AISI 316L Stainless Steel after Magnetoelectropolishing. *Materials* **2009**, *2*, 129–145. [CrossRef]
182. Muthukumaran, V.; Selladurai, V.; Nandhakumar, S.; Senthilkumar, M. Experimental Investigation on Corrosion and Hardness of Ion Implanted AISI 316L Stainless Steel. *Mater. Des.* **2010**, *31*, 2813–2817. [CrossRef]
183. Lodhi, M.J.K.; Deen, K.M.; Greenlee-Wacker, M.C.; Haider, W. Additively Manufactured 316L Stainless Steel with Improved Corrosion Resistance and Biological Response for Biomedical Applications. *Addit. Manuf.* **2019**, *27*, 8–19. [CrossRef]

184. Al-Mamun, N.S.; Mairaj Deen, K.; Haider, W.; Asselin, E.; Shabib, I. Corrosion Behavior and Biocompatibility of Additively Manufactured 316L Stainless Steel in a Physiological Environment: The Effect of Citrate Ions. *Addit. Manuf.* **2020**, *34*, 101237. [CrossRef]
185. Hao, L.; Dadbakhsh, S.; Seaman, O.; Felstead, M. Selective Laser Melting of a Stainless Steel and Hydroxyapatite Composite for Load-Bearing Implant Development. *J. Mater. Process. Technol.* **2009**, *209*, 5793–5801. [CrossRef]
186. Wei, Q.; Li, S.; Han, C.; Li, W.; Cheng, L.; Hao, L.; Shi, Y. Selective Laser Melting of Stainless-Steel/Nano-Hydroxyapatite Composites for Medical Applications: Microstructure, Element Distribution, Crack and Mechanical Properties. *J. Mater. Process. Technol.* **2015**, *222*, 444–453. [CrossRef]
187. Čapek, J.; Machová, M.; Fousová, M.; Kubásek, J.; Vojtěch, D.; Fojt, J.; Jablonská, E.; Lipov, J.; Ruml, T. Highly Porous, Low Elastic Modulus 316L Stainless Steel Scaffold Prepared by Selective Laser Melting. *Mater. Sci. Eng. C* **2016**, *69*, 631–639. [CrossRef]
188. Mondal, P.; Das, A.; Wazeer, A.; Karmakar, A. Biomedical Porous Scaffold Fabrication Using Additive Manufacturing Technique: Porosity, Surface Roughness and Process Parameters Optimization. *Int. J. Lightweight Mater. Manuf.* **2022**, *5*, 384–396. [CrossRef]
189. Jebaraj, A.V.; Ajaykumar, L.; Deepak, C.R.; Aditya, K.V.V. Weldability, Machinability and Surfacing of Commercial Duplex Stainless Steel AISI2205 for Marine Applications—A Recent Review. *J. Adv. Res.* **2017**, *8*, 183–199. [CrossRef]
190. Sup, W.; Sung, M.; Soo, M.; Hyun, M.; Myung, J. Comparative Study on Mechanical Behavior of Low Temperature Application Materials for Ships and Offshore Structures: Part I—Experimental Investigations. *Mater. Sci. Eng. A* **2011**, *528*, 5790–5803. [CrossRef]
191. Peter, L.; Allen, M.; Mark, L.; Martin, L.P. Evaluation of Additive Friction Stir Deposition of AISI 316L for Repairing Surface Material Loss in AISI 4340. *Int. J. Adv. Manuf. Technol.* **2022**, *121*, 2365–2381. [CrossRef]
192. Li, D.; Liu, Q.; Wang, W.; Jin, L.; Xiao, H. Corrosion Behavior of AISI 316L Stainless Steel Used as Inner Lining of Bimetallic Pipe in a Seawater Environment. *Materials* **2021**, *14*, 1539. [CrossRef]
193. Gupta, S.; Singh, D.; Yadav, A.; Jain, S.; Pratap, B. Materials Today: Proceedings A Comparative Study of 5083 Aluminium Alloy and 316L Stainless Steel for Shipbuilding Material. *Mater. Today Proc.* **2020**, *28*, 2358–2363. [CrossRef]
194. Ren, P.; Meng, H.; Xia, Q.; Zhu, Z.; He, M. Tribocorrosion of 316L Stainless Steel by In-Situ Electrochemical Methods under Deep-Sea High Hydrostatic Pressure Environment. *Corros. Sci.* **2022**, *202*, 110315. [CrossRef]
195. Hajian, M.; Abdollah-zadeh, A.; Rezaei-nejad, S.S.; Assadi, H.; Hadavi, S.M.M. Applied Surface Science Improvement in Cavitation Erosion Resistance of AISI 316L Stainless Steel by Friction Stir Processing. *Appl. Surf. Sci.* **2014**, *308*, 184–192. [CrossRef]
196. Bilgili, L.; Mert, T.; Celebi, U.B. Fume Formation Rate of Shielded Metal Arc Welding of Stainless Steel Used in Chemical Tankers In Shipbuilding Fume Formation Rate Of Shielded Metal Arc Welding Of Stainless Steel Used In Chemical Tankers In Shipbuilding. In Proceedings of the 8th International Scientific Conference on Naval, Mechanical and Industrial Engineering, TEHNONAV-2015, Constanta, Romania, 2–4 July 2015.
197. Kaya, Y.; Kahraman, N.; Durgutlu, A.; Gu, E.T. Investigation of the Microstructural, Mechanical and Corrosion Properties of Grade A Ship Steel-Duplex Stainless Steel Composites Produced via Explosive Welding. *Metall. Mater. Trans. A* **2017**, *48*, 3721–3733. [CrossRef]
198. Kaestner, P.; Michler, T.; Weidner, H.; Rie, K.; Bräuer, G. Surface & Coatings Technology Plasma Nitrided Austenitic Stainless Steels for Automotive Hydrogen Applications. *Surf. Coat. Technol.* **2008**, *203*, 897–900. [CrossRef]
199. Karl, A.; Beamer, C. Applications and Design of Low Temperature Surface Hardened Stainless Steel Components in Automotive Applications. *SAE Int. J. Mater. Manuf.* **2016**, *9*, 679–684. [CrossRef]

Disclaimer/Publisher's Note: The statements, opinions and data contained in all publications are solely those of the individual author(s) and contributor(s) and not of MDPI and/or the editor(s). MDPI and/or the editor(s) disclaim responsibility for any injury to people or property resulting from any ideas, methods, instructions or products referred to in the content.